Origami MEMS

Derosh George and Marc J. Madou

1 Introduction

Origami, an ancient Japanese art of folding a single uncut paper to form complex shapes, dates back to the sixth century A. D. It was not very popular back in those days due to the high price of paper. Nevertheless, the art sustained through the generations as a Japanese tradition. There are also some evidences that similar art forms existed in Europe as early as the eighth century. It is not clear, however, if origami in Europe was independently developed or originated also in Japan and found its way to Europe via the famous *silk road*. One of the first written instructions for origami is found in Akisato Rito's 1797 book called "Sembazuru Orikata" (meaning "thousand crane folding"). Although the Origami artwork was practiced in various parts of the world, it was not until the twentieth century, during *Akira Yoshizawa*'s time, that this art form became globalized. *Yoshizawa* published a system of patterns and developed a variant of origami called *wet origami*. *Wet origami* uses a dampened paper instead of a dry sheet of paper to construct more accurate non-geometric origami rather than through mere folding (Fig. 1). In another variation, creation of more complex shapes were made possible through the simultaneous use of multiple sheets of papers in a technique known as modular origami [165]. Later, Demaine and Tachi developed an algorithm to make almost any conceivable polyhedron shapes from a sheet of paper through just folding (Fig. 1) [29, 165]. Collectively, traditional origami, *wet origami,* and *modular origami* can transform simple two-dimensional shapes into three-dimensional shapes of different degrees of complexities [126]. Such origami techniques, from an engineer's perspective, offer some key advantages

D. George · M. J. Madou (✉)

The Henry Samueli School of Engineering, University of California, Irvine, Irvine, CA 92697, USA

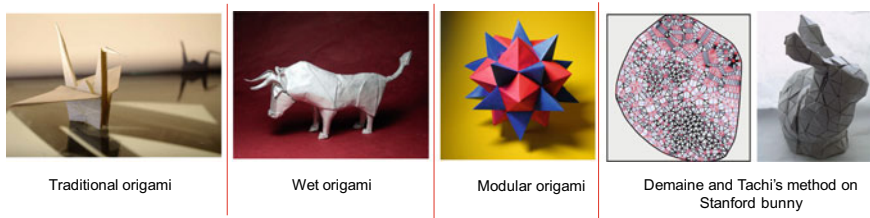e-mail: mmadou@uci.edu

D. George
e-mail: deroshg@uci.edu

| Traditional origami | Wet origami | Modular origami | Demaine and Tachi's method on Stanford bunny |

Fig. 1 Traditional origami (Picture credit: Curt Smith, https://bit.ly/353bCb4), wet origami (Designed by Stephan Weber, https://bit.ly/2MB460z), modular origami (Designed by Tomoko Fuse, https://bit.ly/2t5IsuC), and Demaine and Tachi's method [29]

(i) easy packaging and transportation due to the flat configuration, (ii) high specific strength due to minimal material usage, and (iii) simplicity of construction due to the absence of mechanical components. These advantages inspired engineers of the modern age to translate the origami technique to various engineering platforms, either using paper itself as the material (*paper-based origami*) or with the help of other materials.

A sheet of paper is the raw material, and manual-folding is the construction method in the *paper-based origami* technique. The original purpose of this type of origami was recreational. When adopted for engineering purposes, raw materials and folding strategies had to be rationally adapted for the specific application at hand [65, 118]. Before going into materials other than paper, let us briefly discuss the engineering aspects of *paper-based origami*. For manufacturing *paper-based origami*, folding methods that do not involve manual-folding is necessary. Hand-free folding of paper-based origami shapes is possible via actuation mechanisms that can be implemented on the paper through printing. For instance, folding of a paper can be realized by printing a water-based ink on the paper followed by drying. Drying shrinks the paper locally and results in its folding. The dried paper is stiff enough to sustain a stable folded configuration. Meanwhile, the field of *paper-electronics*, where paper-based electronic systems are studied, offers a host of techniques for incorporating basic electrical elements such as transistors, batteries, and actuators on a *paper-based origami* [33, 55, 83, 127, 131]. *Paper-based origami* has also found application as an inexpensive diagnostic platform. In the year 2007, Whitesides and co-workers from Harvard University introduced a paper-based microfluidic analytic platform using a single piece of patterned paper [107]. Later, the same group presented a more sophisticated form of the paper-based diagnostic platform with a stack of patterned paper layers. Eventually, integration of multilayered paper microfluidics with the origami technique enabled single-step patterning of complex microfluidic systems [171]. This simplification also facilitated easy integration of various components, e.g., a battery, into the system by bringing paper-electronics and paper microfluidics together. In this Chapter, however, we will not be going further into details on paper-based origami structure since these systems are often confined to bigger length scales that are beyond the scope of this chapter. On the other end of the spectrum, molecular methods are used, for example, for making DNA origami. Those techniques are also

excluded here (details on the technique can be found in Hong et al. [53]). What we do focus on here are sheets other than paper for micro-sized origami.

2 Fabrication of Precursor Thin Sheets for Submillimeter Origami

Fabrication methods, including *photolithography, direct writing, and sheet cutting,* are employed (see Table 1) to produce origami precursors at smaller length scales [102], i.e., two-dimensional patterned shapes with submillimeter characteristic lengths. *Photolithography* is one of the most common techniques for microfabrication of planar shapes. In this fabrication paradigm, the desired locations of a planar photopolymer/photoresist layer are chemically modified by irradiating them with light. The locally altered material resulting from the exposure is either more dissolvable in developer or less dissolvable, depending on whether the polymer photoresist is positive (e.g., AZ 1400 series) or negative tone (e.g., SU8 2000 series), respectively (Fig. 2). This technique allows for the fabrication of planar patterns of photopolymers with resolutions well below 100 nm. The patterns obtained can be utilized as a transfer mold/stamp. Alternatively, these photopolymer patterns can act as a mask for selective etching or deposition (Fig. 2). In all these photolithography/photolithography-derived processes, the product is mostly limited to two-dimensional shapes.

While photolithography produces patterned surfaces by removing unwanted parts of the material (a top-down method), the *direct writing* technique creates shapes by adding material to selected locations (Fig. 3) (a bottom-up method). Generally, the dispersion of ink to the selected locations is driven through hydrodynamic forces, electrostatic forces, or mechanical pulling [24, 100, 164]. The resolution of the writing is determined by the size of the line produced by the dispenser, and this size is, in turn, a function of the dispersion technique and other working parameters. The

Table 1 General fabrication methods for thin patterned sheets

| Fabrication methods for thin sheets	Length scale	Specific techniques
Photolithography	100 nm–10 mm	Optical lithography, UV nanoimprint lithography, etc. Other derived techniques include micro-molding, stamping, micro-contact printing, deposition or growth, etching, etc.
Micro/nano writing	10 nm–10 μm	Electrospinning, melt spinning, jet spinning, dry spinning, dip-pen lithography, etc.
Cutting	>10 nm	Laser cutting, focused ion beam, CNC machines, etc.
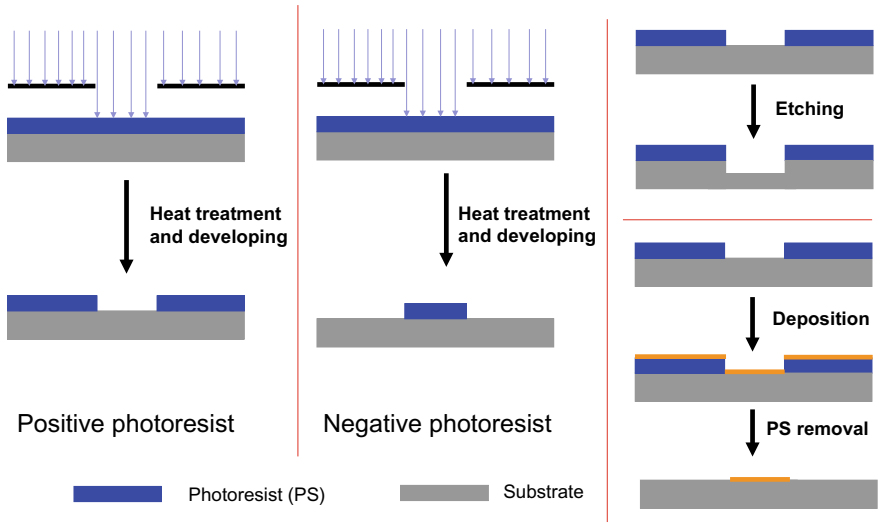
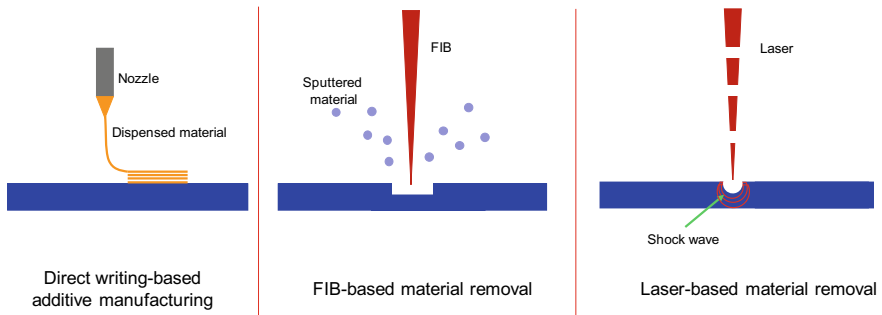**Fig. 2** Photolithography-based fabrication

Fig. 3 Additive manufacturing, and focused ion beam (FIB) and laser-based material removal methods

writing technique can deliver complex three-dimensional shapes by implementing a layer-by-layer writing approach [149]. With the recent advances in the field of direct writing methods, many complex multi-material three-dimensional shapes with high resolution are possible. However, achieving high aspect ratio structures with high fidelity is still a challenge.

Another precursor film fabrication approach is through material removal, such as by *cutting* of thin sheets. Traditional machine-based cutting is widely adopted for the fabrication of various shapes owing to its centuries-old usage. However, this traditional method lacks the capacity to machine tiny two-dimensional shapes. Recently, numerous material removal techniques that utilize non-traditional methods have emerged. For instance, thin sheets can be directly cut using lasers or focused

ion beams (FIB) for forming patterned two-dimensional sheets (Fig. 3). These new techniques made possible resolutions as small as 10 nm.

All three of these fabrication pathways described here—*photolithography, direct writing, and cutting*—have the capability to produce small patterned thin sheets. These patterned sheets, if folded, could create tiny three-dimensional shapes. Such three-dimensional structures and systems of submillimeter scales are generally referred to as *Origami MEMS (Microelectromechanical systems)*. Folding in such a small length scale demands creative folding strategies since manual-folding used in traditional paper-based origami is not a feasible choice for submillimeter origami shapes. In the following section, different approaches to folding sheets in the submillimeter regime are discussed.

3 Folding Strategies for Origami MEMS

Here, we examine various strategies for folding submillimeter and sub-micron scale patterned thin sheets for origami shapes. Logical approaches to accomplish folding in the submillimeter regime include (i) borrowing existing folding strategies from a larger length scale, or (ii) mimicking folding mechanisms found in nature. Bending and buckling tactics are adopted to transform simple two-dimensional shapes to complex three-dimensional shapes in the submillimeter length scale. The bending of a sheet takes place when it experiences an out-of-the plane moment (Bending moment). Buckling, on the other hand, is a result of a compressive force on a slender object. Both bending and buckling on a sheet material is generally realized via two different methods: (1) by introducing a non-uniform material property across the sheet thickness followed by a trigger, or (2) by applying an external force to materials having a uniform property (Fig. 4). Generally, for the first case, a mismatch in the deformations at different locations of cross-sections across the thickness (a strain mismatch) causes bending or buckling. The required strain may be induced via
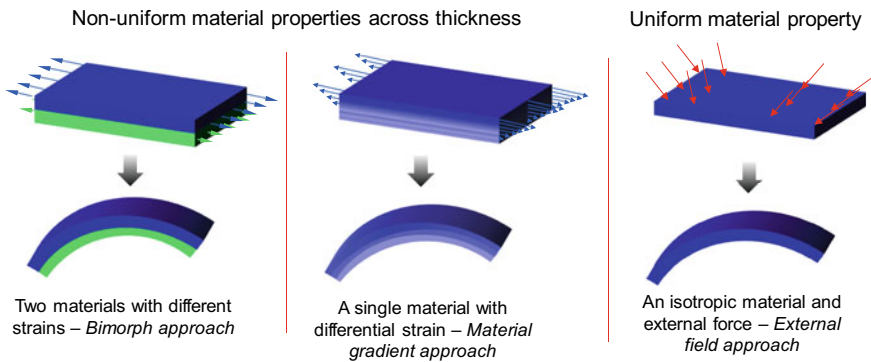

Fig. 4 Bimorph approach, material gradient approach, and external field approach

swelling, shrinkage, thermal expansion, piezoelectric effect, configuration change in a liquid crystal elastomer, or shape memory effect (Table 2). In the second case, an external force prompts bending or buckling of sheets that are isotropic in nature. Driving forces of such geometrical transformation include surface tension-based actuation, magnetic actuation, mechanical actuation, or electrical actuation (Table 2).

Bending and buckling are achieved in the submillimeter length scales using the following strategies (Fig. 4).

(1) By introducing different strain values on two attached sheet materials—*Bimorph approach*.
(2) By introducing differential strain across the thickness of a single material by designing different material properties across its thickness—***Material gradient approach***.
(3) By using external fields on a material with uniform properties across the thickness—***External field approach***. (Note: External fields may be required for the activation of both #1 and #2, but the material property across the thickness is not uniform in either of them.)
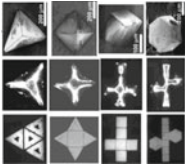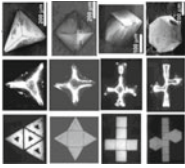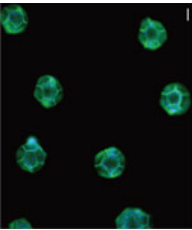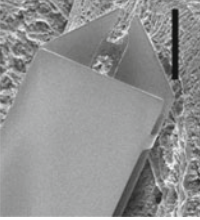
3.1 Bimorph Approach

Materials often display deformation when heated. Generally, dimensional changes generated in a material due to changes in temperature are homogeneous, leading to simple stretching or compression. However, when two such sheets (Generally, metals in the case of larger length scales) having distinct thermal expansions are bonded together (e.g., *bimetallic strip*), the resulting structure bends upon heating because of their strain mismatch [32]. The bending is such that it forms a convex curvature on the side having material with relatively higher thermal expansion material. Curvature formation by heating of bimetallic strips is one of the conventional approaches for bending thin constructs at scales larger than a millimeter (Fig. 5). The curvature, κ, is expressed based on Timoshenko's plate theory [146] and is given as follows.

$$\kappa = \frac{6\Delta\alpha(1+m)^2}{h\left\{3(1+m)^2 + (1+mn)\left(m^2 + \frac{1}{mn}\right)\right\}} \tag{1}$$

where $\Delta\alpha$ is the difference in thermal expansion coefficients of the two materials, m is the thickness ratio between them, and n is the stiffness ratio of the two materials. Although the same concept of bending driven by distinct strains of two materials (bimorphs) can be implemented for the microfabrication of bent structures, the execution of the idea at that length scale must adopt various crafty new ways. Driving forces relevant for bending sheets of micron length scales include *residual stress, swelling, liquid crystal alignment, and shape memory effect*. The general strategy is to attach these active materials to another inactive substance, followed by actuation/trigger (*Unimorph*). Alternatively, both the sheets could be active materials (*Bimorphs*).

Table 2 Different actuation mechanism for origami fabrication and their details

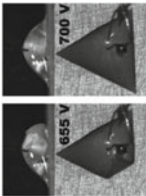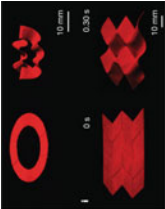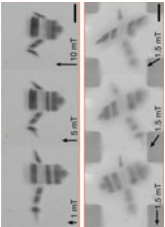| Actuation mechanisms	Size of origami	Advantages and disadvantages	Reversible/Irreversible
Capillary force	100 nm–1000 μm	Advantages – Inexpensive fabrication Disadvantages – Pairing of droplets and sheets demands multilayer fabrication – Difficulty making complex shapes – Elastomers return to their original shape	Reversible or irreversible
e.g.			
 [45]	 [77]	 [153]	 [20]
[45] (Copyright 2002 by John Wiley & Sons, Inc. Reproduced by permission of John Wiley & Sons, Inc.) [77, 153] (Reprinted with the permission of AIP Publishing) [20] (Copyright 2009 American Chemical Society) [38, 44, 88, 93, 117, 121]			
Electric field/magnetic field	100 μm–10 mm	Advantages – Excellent temporal control over the folding – Quick response – Easy manipulation – Wireless control – Nanorobot fabrication (Magnetic) Disadvantages – External system to control the device	Reversible

(continued)

Table 2 (continued)
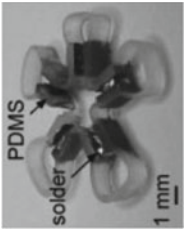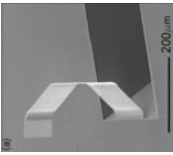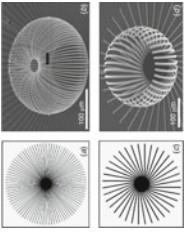
Actuation mechanisms	Size of origami	Advantages and disadvantages	Reversible/Irreversible
e.g.			
[119]	[71]	[170]	[25]

[119] (Reprinted with permission from the Royal Society of Chemistry) [71] (Reproduced by permission from Macmillan Publishers Ltd: Nature, copyright 2018) [170] (Copyright 2019 by John Wiley & Sons, Inc. Reproduced by permission of John Wiley & Sons, Inc.) [25] (Reproduced by permission from Macmillan Publishers Ltd: Nature, copyright 2018) [141, 161]

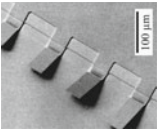| Residual stress	>10 nm	Advantages – High accuracy – High resolution – Bending can be controlled by the thickness of the layer. – Microfabrication is possible Disadvantages – Complex multilayer fabrication	Reversible or irreversible
e.g.			

(continued)

Table 2 (continued)

Actuation mechanisms	Size of origami	Advantages and disadvantages	Reversible/Irreversible
[152]	[13]	[5]	[112]

[152] (Reprinted with the permission of AIP Publishing) [13] (Copyright 2005 by John Wiley & Sons, Inc. Reproduced by permission of John Wiley & Sons, Inc.) [5] (Reprinted with the permission of AIP Publishing) [112] (Reproduced with permission. © IOP Publishing. All rights reserved) [9, 21, 23, 76, 97, 98, 112, 133, 151, 176]

Actuation mechanisms	Size of origami	Advantages and disadvantages	Reversible/Irreversible
Swelling (solvent transfer, heat-assisted, pH-responsive, etc.	~100 μm	Advantages – Large deflection – Various triggered actuation – Biocompatibility – Biodegradability Disadvantages – Reduced stiffness – Slow response	Reversible

e.g.

(continued)

Table 2 (continued)

Actuation mechanisms	Size of origami	Advantages and disadvantages	Reversible/Irreversible
 [47]	 [7]	 [136]	 [140]
Shape memory effect e.g.	~1 mm	Advantages – Good mechanical properties – Relatively faster response Disadvantages – Material response depends on the original configuration – Low efficiency – Difficulty to microfabricate – Difficulty to make complex structures	Reversible or irreversible

[47] (Copyright 2009 American Chemical Society) [7] (Copyright 2010, reprinted with permission from Elsevier) [136] (Reprinted with permission from the Royal Society of Chemistry) [140] (Reproduced by permission from Macmillan Publishers Ltd: Nature Materials, copyright 2016) [69, 74, 85, 138, 166, 175]
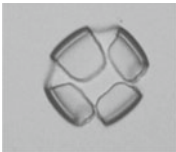
(continued)

Table 2 (continued)

Actuation mechanisms	Size of origami	Advantages and disadvantages	Reversible/Irreversible
D [147]	[106]	[35]	[54]
[147] (Reproduced with permission. © IOP Publishing. All rights reserved) [35, 106] (Reproduced with permission. © IOP Publishing. All rights reserved) [54] (Reproduced with permission. © IOP Publishing. All rights reserved) [31, 142, 144, 157]			
Liquid crystal	~1 mm	Advantages – Fast response – Different triggers Disadvantages – Difficulty to microfabricate	Reversible
e.g. [99]	[81]	[14]	[168]

[99] (Copyright 2018 by John Wiley & Sons, Inc. Reproduced by permission of John Wiley & Sons, Inc.) [14, 81] (Reprinted with permission from the Royal Society of Chemistry) [168] (Reprinted with permission from the Royal Society of Chemistry) [86, 158]

Table 2 (continued)

Actuation mechanisms	Size of origami	Advantages and disadvantages	Reversible/Irreversible
Buckling	<1 mm	Advantages – Fabrication of complex configurations Disadvantages – Less explored – Difficult to control (Multiple stable configurations)	Irreversible

e.g.

[139]

[162]

[40]

[139] (Reproduced by permission from Macmillan Publishers Ltd: Nature Nanotechnology, copyright 2006) [162] (Copyright 2016 by John Wiley & Sons, Inc. Reproduced by permission of John Wiley & Sons, Inc.) [40] (Reproduced by permission from Macmillan Publishers Ltd: Nature Materials, copyright 2016) [130, 160]

Fig. 5 Bimetallic strip
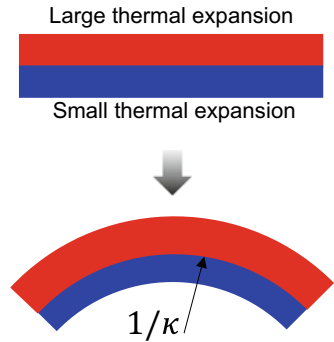
The term *bimorph* is often used as a more generalized term encompassing both *uni-* and *bimorph*s. We will be following the same convention from here onwards.

3.1.1 Fabrication Strategies for Curved Shapes Using a Bimorph Approach

Rational exploitation of *residual stress, swelling, configuration change in liquid crystal elastomer, or shape memory effect* results in bent shapes (Fig. 6). In microfabrication, material deposition often entails compressive or tensile *residual stress* within the layers of materials. This *residual stress* is, generally, considered detrimental for microfabrication since it acts as a bottleneck for some of the traditional fabrication processes since a large amount of such pre-stress leads to cracking of the films or even of the substrate. Conversely, the same pre-stress may be able to generate a bending moment capable of forming origami shapes if adjoined with another material having different internal stress. For instance, one of the ways to grow SiO_2 on silicon is by thermal oxidation. This thermal growth produces a SiO_2 layer with compressive stress. When a metal with lesser compressive stress is deposited on top of this pre-stressed SiO_2 layer, and then the bilayer is released from the silicon, the strain mismatch results in the bending of this *bimorph* [112]. Similarly, chromium deposition also introduces *residual stress*. Consequently, a bilayer of chromium (Cr) and copper (Cu) exhibits bending as soon as it is released from the supporting structure. As an extension of this bimorph approach, bending in both directions can be achieved by depositing copper and chromium in a Cr/Cu/Cr arrangement [9]. The bending direction, in this case, is dictated by the thicknesses of the patterns of the chromium layer on the top and on the bottom.

Nature presents a variety of movement mechanisms in plants by exploiting *swelling* caused by water. Generally, a gradient in the solvent concentration across a cell wall leads to water intake by the cell through osmotic pressure build-up. Intake of water, in turn, leads to their *swelling*, and this can trigger movement in
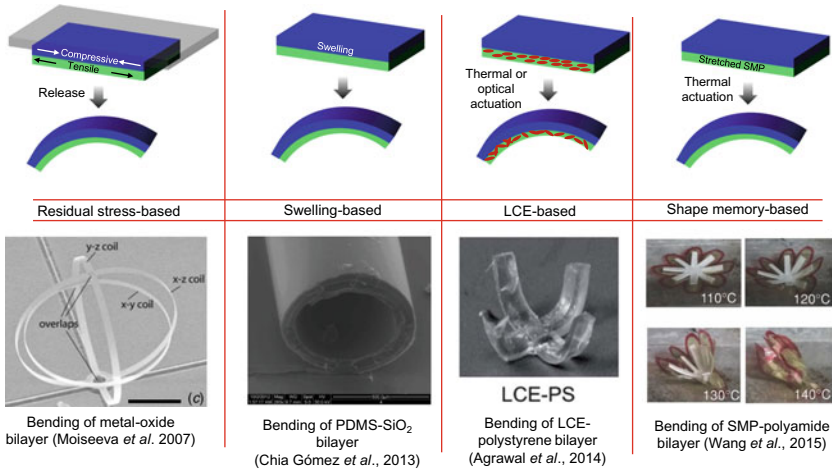
Fig. 6 Implementation of bimorph approach to obtain *bending* using residual stress (Reproduced with permission. © IOP Publishing. All rights reserved) [112], swelling/shrinking (Republished with permission of the Royal Society of Chemistry; permission conveyed through Copyright Clearance Center, Inc.) [19], liquid crystal elastomer (Republished with permission of the Royal Society of Chemistry) [1], and shape memory polymers [157]

plants [68]. Among various examples from nature, one of the most studied is the bilayer design that causes the release of ripe seed from *conifer cones* [27]. A technique emulating such bending can be adopted for the fabrication of small origami shapes [3]. Hydrogels and certain other polymers are capable of absorbing solvents. Temporal and spatial control of this absorption and the resulting swelling of polymers enable bending and folding in those precursors (Fig. 6) [59]. Additional control over the bending or folding may be achieved by designing materials that respond to stimulations such as a change in pH, temperature, enzyme concentration, light intensity, electric field, and solvent concentration [7, 91, 96, 132, 148, 156].

A *liquid crystalline elastomer* (LCE), another type of active material, is synthesized by aligning liquid crystals (LCs) inside a cross-linked polymer matrix by means of mechanical, surface, or chemical forces [115]. The aligned LCs enhance the stiffness along the length of their orientation. On the other hand, when transformed into a randomly oriented configuration, the misalignment is manifested at the macroscale as a contraction of the LCE along the initial alignment direction (Fig. 7). This material deformation characteristic of an LCE makes it possible to fabricate three-dimensional shapes that are activated through different mechanisms. One such method utilizes a light-sensitive molecule called Azobenzene (AZ). AZ exhibits *cis-trans* isomerization under the influence of UV light, where *trans*-AZ has a rod shape and lets the LCE keep its ordered shape, *cis*-AZ has a bent configuration, and its presence adversely affects the ordered structure of the LCE [87]. Disorder in an LCE, as mentioned earlier, leads to the deformation of the material. Therefore, attaching this kind of LCE to an inactive material and then shining UV light invokes the bending of
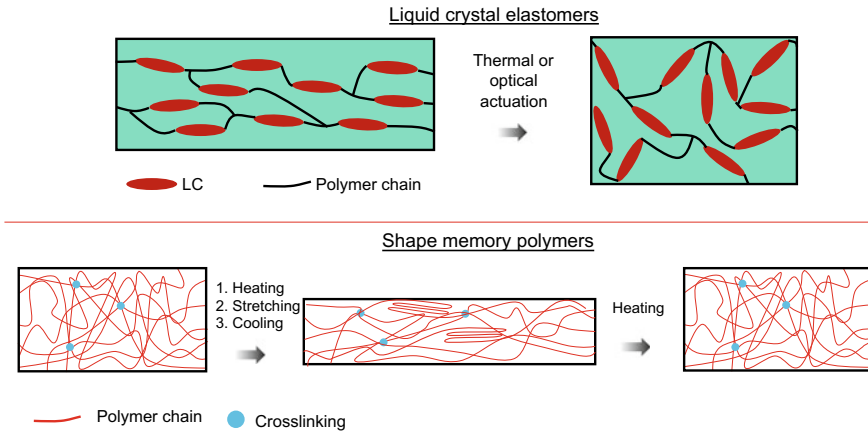
Fig. 7 Working principle of liquid crystal elastomers and shape memory polymers

this assembly (Fig. 6). Similar to this chemically engineered degree of crystallinity, mechanical forces can also induce alignment inside an LCE [28]. In the event of heating beyond its LC–isotropic phase transition temperature, the material loses its alignment, leading to mechanical deformation.

Shape memory is another actuation mechanism that can be employed for bending. *The shape memory effect* is a material's ability to remember a configuration and return to that state upon actuation. Among various materials showing shape memory effects, shape memory alloys (SMAs) and shape memory polymers (SMPs) are the two major categories used in origami fabrication. SMA displays the shape memory effects because of its microstructure. For instance, NiTi, an SMA, has two stable crystal structures: *austenite* (stable at high temperatures) and *martensite* (stable at low temperatures). A deformation applied in the SMA's *martensitic* state is reversed upon converting it to *austenite*. Generally, SMAs are stretched in the *martensitic* state. The stretched SMAs contract when heated. This contraction results in bending in a bilayer, as depicted in Fig. 6. SMA increases the flexibility associated with system design since heating required for the actuation can be induced simply by applying a Joule heating current. Wireless powering with the help of an electromagnetic field is sufficient to attain the folding of centimeter-scale origami [15]. Despite these advantages, SMA is rarely used in smaller length scales due to the difficulty associated with its micropatterning.

SMPs function based on an entirely different principle [11, 89, 124]. SMPs are generally amorphous polymers (polymer chains are randomly oriented) with restricted polymer chain mobility at room temperature. When they are heated above a specific transition temperature, the polymer chains attain more flexibility and are able to twist and rotate. At this stage, deformation is induced easily due to the enhanced mobility of the chains (Fig. 7). The polymer is then cooled down, and the deformation is temporarily locked down through physical or chemical interactions of

the chains. When reheated, the original shape is recovered. Therefore, bending can be induced with such a deformed SMP that abuts an undeformed SMP sheet (Fig. 6).

Although we mentioned various techniques where strain mismatch is used for bending, it must be noted that not any combinations of two materials that are having different strains offer a uniform bending toward one direction. A thin and stiff material on top of soft and thick material can result in wrinkled shapes on the thin material [18]. This kind of deformation is not of interest at the moment for designing origami fabrication processes. Another peculiar case is when the bilayer is longitudinal rather than along thickness. The differential strain along the lateral dimension can lead to curled shapes [17, 51, 69].

3.1.2   From Bending to Folding Using Bimorph Approach

A *fold* features a large curvature over a length that is considerably smaller than the overall size to the sheet [84]. Two typical design strategies are followed for fabricating a single fold shape and are depicted in Fig. 8. In the first strategy, the actuator is present only at the fold, and its deformation induces folding on the sheet assembly. The same technique can also be utilized for designing the timely folding of a bimorph. For instance, the application of a phase transforming or stiffness changing polymer at the folds of the bimorph can prevent the spontaneous folding of residual stress-based bimorphs and instead enables a controlled bending of the film driven by softening of the polymer with an appropriate trigger [8, 80]. In the second case, although the actuator is present along the whole length of the sheet, the bending is majorly focused on the fold region. Such local bending is possible by increasing the bending stiffness
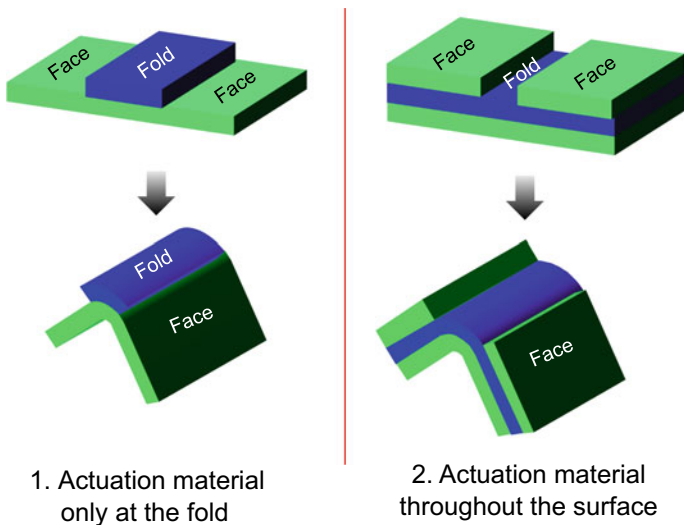

1. Actuation material
only at the fold

2. Actuation material
throughout the surface

Fig. 8 General *folding* strategies

of the faces (shown in Fig. 8). A typical example is a strip of bimorph with two rigid panels at the face regions. The bending predominantly happens at the folds since the faces are reinforced with an additional layer of material. As an extension of this folding technique, bi-directional folding (mountains and valleys) can be achieved if a soft material is sandwiched between two sheets having patterned openings on the top and bottom layers. This ability to fold in both directions allows for the fabrication of complex shapes. In one of the demonstrations by Na et al., such a tri-layer design was used to make a "crane" shape at micron length scale [114] (Fig. 9). The soft hydrogel sandwiched between two rigid layers had an elastic modulus two orders of magnitude less than the ones that were sandwiching it. This difference in their moduli ensured that the deformation led to *folding*, but not *bending*. It must be noted that, alternatively, a *local actuation* of the bimorph at the folds can also result in folding.

We mentioned earlier that bimorphs, without any other modifications, results in *bending*. An exception to such uniform bending is the hierarchical *bending* of polymer bilayers, which leads to *folding* [137]. Initially, when the absorption of water is activated at the edges of the bimorph, the bending occurs only at the borders of the pattern. This localized absorption and swelling lead to a tube formation at the edges. High rigidity of such tubes restricts the subsequent bending only to the

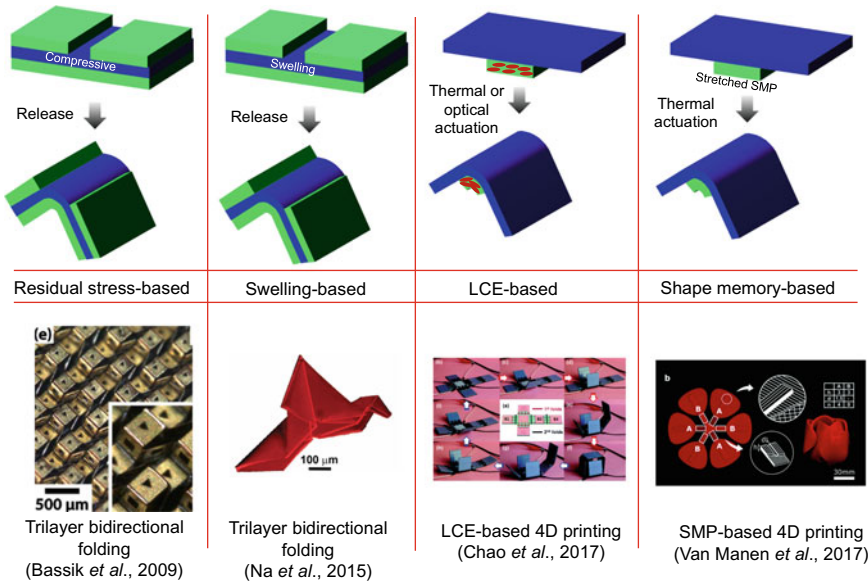**Fig. 9** Implementation of bimorph approach to obtain *folding* using residual stress (Reprinted from Bassik et al. [9], with the permission of AIP Publishing), swelling/shrinking [114] (Copyright 2014 by John Wiley & Sons, Inc. Reproduced by permission of John Wiley & Sons, Inc.), liquid crystal elastomer [168] (Reproduced with permission from The Royal Society of Chemistry), and shape memory polymers [145]

intersections of those tubes. This localized bending enables folding without any additional patterning [136] (Table 2).

As far as the execution of the bimorph-based folding strategies is concerned, most of the examples discussed so far were based on *lithography*. For patterning some of the materials, we may have to rely on other techniques such as *direct writing*. Let us revisit the direct writing-based additive manufacturing method that was mentioned earlier in this chapter. It is a process of making complex three-dimensional shapes by *layer-by-layer* writing. In this technique, the volume of the target shape determines the time required for the fabrication, irrespective of whether a structure is hollow or solid. Consequently, fabrication time for a two-dimensional patterned origami precursor sheet is an order of magnitude less than the time required for the fabrication of corresponding three-dimensional shape. Therefore, folding of two-dimensional sheets is preferred over the direct writing of the corresponding three-dimensional shapes, as far as the throughput of fabrication is concerned. A further improvement could be made by introducing 4D printing, where the morphing of the shape with respect to time is the fourth degree of freedom (Fig. 9). This kind of morphing can reduce the production time and enables an extra degree of freedom, giving rise to *free-form* manufacturing. This kind of manufacturing is generally realized by incorporating active materials such as LCE and SMP in additive manufacturing (multi-material printing), followed by actuation [42].

Incorporation of the LCE into direct writing technologies was made possible with a relatively less viscous LCE ink. Low viscosity simplified the writing process and helped introducing the required degree of molecular alignment in the resulting precursor pattern. Shear-thinning during direct writing causes the needed alignment of liquid crystals. The folding action can be initiated through Joule heating of an embedded wire inside a bimorph containing LCE [168].

Multi-materials polymer 3D printers that are compatible with SMPs can fabricate foldable multi-material precursors. SMP is printed only on one side of the fold region to introduce a strain difference favorable for folding [41]. At a temperature higher than the transition temperature, the printed sheets are stretched and brought to a temperature lower than the transition temperature. When cooled, the SMP retains its original shape, but the elastomer to which it is attached does not. This difference in strain results in the bending of the sheet. When this bent shape is heated again, SMP goes back to the original shape leading to the flattening of the sheet. Printing at a temperature above the material's transition temperature can simplify the overall process even further as shown by Van Manen et al. [154]. During the printing, the ink is extruded. This stretching is memorized by the polymer and leads to the morphing when reheated (Fig. 9).

3.2 Material Gradient Approach

Fabrication of bimorphs requires either multilayer photolithography or a multi-material writing, increasing the complexity of the process. Moreover, the strain
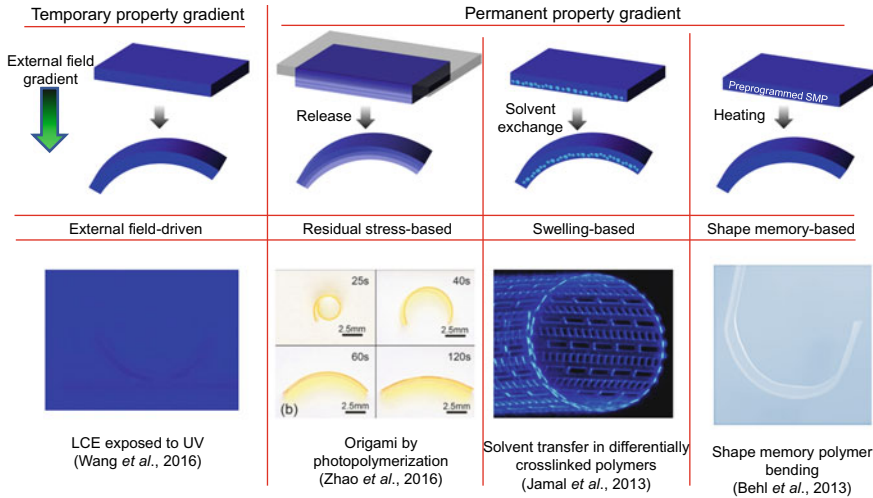
Fig. 10 Implementation of material gradient approach to obtain *bending* using a gradient in the external field [158], residual stress [174] (Copyright 2017 by John Wiley & Sons, Inc. Reproduced by permission of John Wiley & Sons, Inc.), swelling/shrinking [64] (Reproduced by permission from Macmillan Publishers Ltd: Nature Communications, copyright 2013), and shape memory polymers [10] (Copyright 2013 by John Wiley & Sons, Inc. Reproduced by permission of John Wiley & Sons, Inc.)

mismatch that drives the morphing of the bimorph may cause occasional delamination at the interface of the two materials. Having a smooth property gradient is the remedy for such problems that arise from a large strain mismatch (Fig. 10).

3.2.1 Fabrication Strategies for Curved Shapes Using Material Gradient Approach

Material property gradient within a sheet material can be categorized into two types: (i) *transient property gradient* and (ii) *permanent property gradient*. A *transient property gradient* is attained via reversible molecular rearrangement. An LCE sheet containing AZ, when irradiated, experiences different degrees of rearrangements at its polymer matrix across its thickness, with the side closer to the light source experiencing more changes. The difference in molecular rearrangement results in a gradient in deformation with more contraction on the side closer to the light source, leading to a bent shape. This type of tactic may be applied for swelling-based bending too [49, 52, 123]. A concentration gradient of absorbing molecule in the medium results in a difference in the absorption across the cross-section of the sheet. However, these techniques are rarely utilized for the fabrication of complex origami shapes due to its unidirectional bending (Note: here, external field changes the material property across the thickness unlike *external field approach* that we are going to discuss later,

where field induces a bending moment without interfering with the material properties). Therefore, a property gradient that is permanently embedded in the material is preferred to a method that purely relies on an external field to fold origami. A permanent property gradient across the thickness of a sheet is fulfilled during its synthesis [75, 120]. Fabrication of photopolymer sheets with varying *crosslinking density* is one of such synthesis methods. Photopolymers crosslinks when exposed to light. The *crosslinking* occurs first in the region that is closer to the light source. For explaining the process, this region is referred as the first layer, even though the *crosslinking* is not really a layer-by-layer process. The polymer undergoes shrinkage as a result of the crosslinking. As far as the first layer is concerned, the polymer is free to shrink in every direction. However, once a solidified layer is formed, the contraction of the subsequent layers would be constrained by the first layer. This constraint results in residual stress inside the material. The *residual stress* this region experiences is analogous to a stretched band. If this residual tension is released, the sheet will bend as shown in Fig. 10. This photopolymer-based execution of the gradient approach, *frontal photopolymerization*, can create complex shapes having millimeter length scale [173]. A similar type of bending can be achieved using direct writing techniques too. Like the *frontal photopolymerization*-driven bending, the residual strain build-up during the writing of the second layer can lead to the bending of the film.

The degree of crosslinking across the thickness of a photopolymer reduces with the distance from the light source. This crosslinking density gradient directly correlated to the porosity density inside its polymer matrix. Specifically, a less cross-linked SU8 sheet possesses a relatively more porosity compared to a more cross-linked sheet. Porosity in a material allows for the absorption of various solvents by the substance. The more porosity the material has, the more solvent it absorbs. Consider a thin sheet with a crosslinking density gradient varying from a high level of crosslinking on the top to a low level of crosslinking on the bottom. If one fabricates such flat sheets with absorbed liquid (e.g., developer solution) inside them, the bending of the faces occurs toward the bottom surface when the solvent is removed. The cause of the bending is attributed to the shrinkage resulting from the removal of the large quantity of the solvent from the highly porous bottom surface of the sheet [63]. Please keep in mind that the reported fabrication based on this technique showed only a reversible bending of the SU8 film since nothing prevents the folded structures from going back to the original shape when placed inside the same solvent again. We will discuss a strategy to make permanent folding later in this chapter.

In the case of an SMP with a preprogrammed bending trained on it, the sheet bends to the "memorized" shape upon heating. Unlike in the case of bimorph, where the linear deformation of the SMP bends a bilayer sheet consisting of the polymer and another material, bending, in this case, is not assisted by a second material.

3.2.2   From Bending to Folding Using Material Gradient Approach

Localized modification of material properties is easy to achieve with photopolymers by selectively illuminating the polymer sheet. In one of the methods, selective
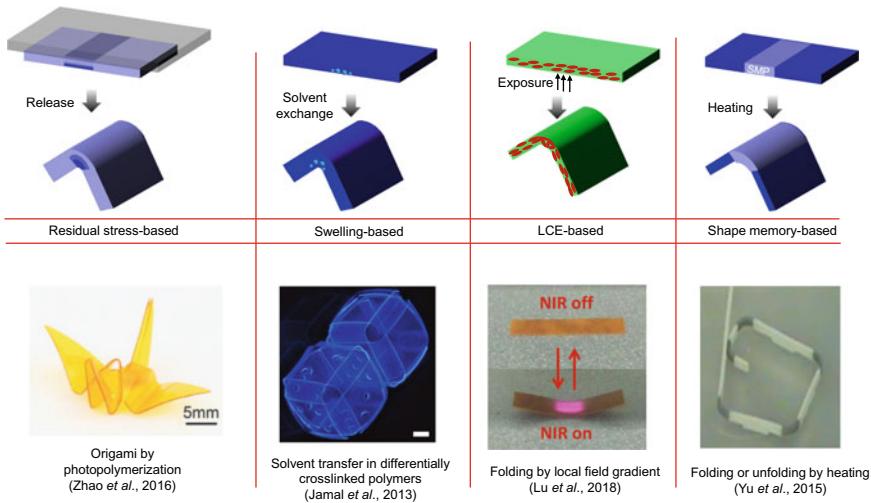
Fig. 11 Implementation of material gradient approach to obtain *folding* using residual stress [174] (Copyright 2017 by John Wiley & Sons, Inc. Reproduced by permission of John Wiley & Sons, Inc.), swelling/shrinking [64] (Reproduced by permission from Macmillan Publishers Ltd: Nature Communications, copyright 2013), liquid crystal elastomer [99] (Copyright 2017 by John Wiley & Sons, Inc. Reproduced by permission of John Wiley & Sons, Inc.), and shape memory polymers [167] (Copyright 2015, with permission from Elsevier)

exposure was performed such a way that it concentrates the residual stress from the aforementioned sequential crosslinking to the fold region, leading to folding (Fig. 11). Selective irradiation, in certain other photopolymer material, results in stress relaxation inside the material due to a polymer network rearrangement [90]. Mechanical and optical stimuli have been combined in a technique called *photo-origami* to exploit this stress relaxation to accomplish folding [128]. In this method, the sheets are stretched perpendicular to the length of the fold, followed by a UV exposure at the fold region. By exposing the fold region of a stretched film, local-ized stress relaxation can be controlled. Exposure energy density varies across the thickness of the sheet. The side closer to the light source experiences a higher energy density. As a result, the irradiated side of the film experiences relatively more stress relaxation, causing local bending. The porosity density gradient that emerges from a differential crosslinking can also be focused on the fold region to achieve folding at submillimeter scales (Fig. 11).

In another related light-based folding, sequential folding in mesoscale is achieved with *Shrinky dinks*, by printing the folds with inks of different colors followed by exposure to high-intensity light [97]. Unlike the previously mentioned photosensitive materials, here, the bending occurs due to the local heating of the material. The absorption wavelength by the ink depends on its color/absorption property. Absorbed light heats up the fold. Therefore, folds having different colors can be locally heated when they are exposed to the complimentary spectrum that they can absorb. *Shrinky*

dinks contract considerably upon heating because of strain release, and as a result, folding of the sheet happens. Instead of colored inks on the hinges, a graphene ink may be deposited to bend *Shrinky dink* material to actuate the folding with microwave [26]. When exposed to microwave, since graphene is not transparent to microwave, the sheet is locally heated. Like the previous case, this local heating results in bending. However, the orientation of the fold with respect to the wave affects the folding of the material, limiting the versatility of the technique. In nanoscale, a focused ion beam (FIB) is used for the fabrication of folded shapes. FIB, when bombarded with the nanofilm, induces tensile or compressive stress on the film depending on the operating parameters. Gallium ion from FIB when colliding with the film can remove atoms from the gold film. The vacancies formed via this bombardment lead to grain coalescence and as a result, residual tensile stress on the top layer of the film, as illustrated in Fig. 12. This leads to the bending of the thin film [133].

Heating-based folding can be induced in an LCE by locally heating the sheet beyond its transition temperature with IR irradiation (Fig. 11). The side that is heated experiences a shrinkage due to the molecular rearrangement, leading to the bending of the LCE sheet. While folding in LCE is achieved through IR illumination of an isotropic material, an SMP-based folding requires local preprogramming of an SMP. A direct writing technique may be employed to fabricate folds with SMP and the faces with an inactive material. By training this SMP-made fold region, folded origami can be obtained (Fig. 11).

3.3 *External Field Approach*

Here we discuss a new approach where bending of a sheet is carried out without changing its properties across the cross-section, contrasting previously discussed cases where the material properties of the sheets are tuned to induce bending. Various forces, including capillary, magnetic, and external compressive forces, can be the cause of bending in an external field approach. Since the external field approach involves different forces, it is essential to discuss them briefly before delving into the fabrication aspects of it.

Capillary effects scale favorably for the micron-scale actuation. A comparison of the body forces ($\rho g l^3$) with the surface tension forces (γl), where l is the length scale, γ is the surface tension, ρ is the density, and g is the gravitational constant, reveals that the surface tension effects dominate in a smaller length scale. Therefore, surface tension can act as an actuation mechanism for micro-origami fabrications. Nature takes advantage of this fact, as observed in the case of the drinking mechanisms of both phalaropes and hummingbirds. For a phalarope, this heightened effect of surface tension at small scales is a way to accomplish, a gravity-defying intake of prey-laden water toward its mouth. A Hummingbird's tongue exploits the surface tension to close lamellae on its tongue to entrap honey at each of its dips into honey-filled flowers. Here, the tongue closes because of the interaction between the soft
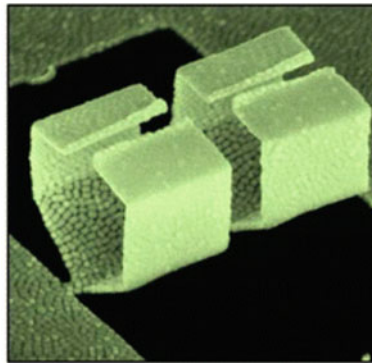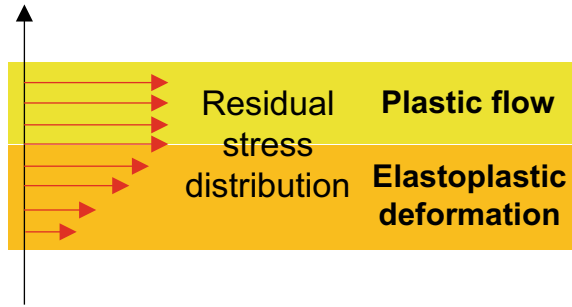
FIB (Si *et al.*, 2014)

lamellae and the honey. This bending phenomenon, surface tension-driven bending of the soft materials, is known as *elastocapillary* bending.

Droplets most often assume a spherical cap shape on a solid or a liquid surface to minimize the total surface energy. A droplet on a hard surface has three different surface energies associated with it: surface energy due to the air–liquid, solid–liquid, and solid–gas interfaces. For a droplet-surface-gas system, if the energy of liquid–gas and solid–liquid interfaces is very high as compared to the other interface, the droplet forms a complete sphere to minimize the total energy. On the other hand, if the surface energy of the solid–liquid and liquid–gas is sufficiently small, the liquid spreads on the surface to avoid having the high energy offered by the solid–gas interface. In a case that is midway between these two cases, the droplet forms part of a sphere. Now imagine having a droplet on a thin sheet. The system has an extra option to wrap the sheet around the droplet to minimize the liquid–gas interfacial energy at the expense of the bending energy of the sheet. For a sufficiently thin sheet, this increase in energy is less than the reduction in surface energy. As a result, bending occurs (Fig. 13). Length scale below which the effect of capillary forces becomes significant is found by comparing the Laplace pressure, γ/l with the hydrostatic pressure, $\rho g l$, where l
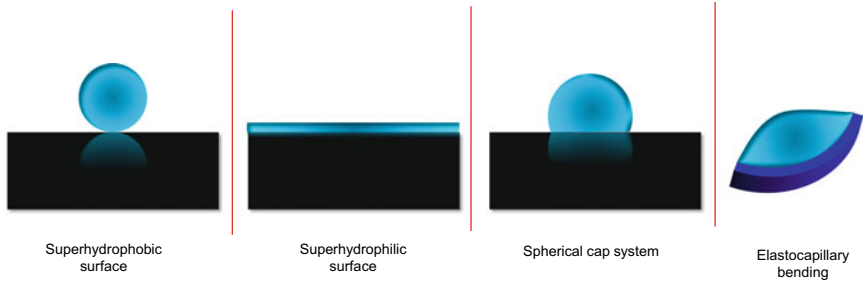
Fig. 13 Different configurations resulting from droplet-surface interactions

is the length scale, γ is the surface tension, ρ is the density, and g is the gravitational constant and is given by the capillary length, $l_c = \sqrt{\frac{\gamma}{\rho g}}$. For a significant bending, the curvature can be assumed to be of the order of $1/l$. Therefore, the bending energy density ($E_B = \frac{1}{2} B \kappa^2$) scales as $Eh^3/24(1 - \nu^2)/l^2$. The length scale at which the surface energy density of a droplet, γ, becomes significant is then obtained by equating the bending energy density (E_B) with it and is given by *elastocapillary* length $L_{EC} = \left(\frac{Eh^3}{24(1-\nu^2)\gamma} \right)^{\frac{1}{2}}$.

Controlled bending of a thin sheet using *elastocapillary effect* is achieved either with different droplet sizes or by adjusting the interfacial tensions of the sheet substrate. Droplets with a characteristic length too small or too big compared to the thin sheet do not bend the sheet significantly. In the case of a small droplet, energy gain would be negligible, and for a big droplet, bending of the sheet would require a significant deformation of the droplet, an energetically expensive process. Applying an electric field to the droplet changes the surface energy of the droplet. This change is manifested as change in the angle that the droplet makes with the substrate. When an electric field is applied to the droplet system, the energy associated with it is modified with additional electrostatic energy which is of the order of $\frac{\epsilon L^2 V^2}{2(d+h)}$, where ϵ is the dielectric constant, d is the insulating layer thickness, V is the voltage, h is the thickness of the sheet, and L is the length of the sheet. Comparing the electrical energy with the surface energy would give an idea about the order of magnitude of the voltage at which the contact angle is significantly affected by it and is given by $V \sim \sqrt{\frac{\gamma(d+h)}{\epsilon}}$. Alternatively, the energy of the solid surface can be changed for controlling the folding angle [105, 119]. Oxygen plasma treatment is usually used for controlling the surface energy of the solid.

The magnetic effect can be utilized for causing deformation in materials. Elastomeric films embedded with magnetic particles can be magnetically controlled. An external magnetic field, B forces the particles to orient along its direction [56].

Buckling occurs when a thin sheet is subjected to a compressive force. Energy density E_s of a compressed flat plate of a thickness t and a length L is proportional to $t \left(\frac{\delta}{L} \right)^2$, where 2δ is the displacement by which it is compressed. Pure bending energy E_B is, on the other hand proportional to $t^3 \kappa^2$, where κ is the curvature of the

flat plate. Thicker films experience a uniform compression across the cross-section of the plate. However, as the thickness reduces, the bending of the sheet becomes energetically more favorable. Therefore, thinner plates experience out of the plane buckling when compressed.

3.3.1 Fabrication Strategies for Curved Shapes Using External Field Approach

Researchers from École Polytechnique, France, made complex three-dimensional shapes by applying capillary force by placing a drop of water on top of a pre-cut patterned two-dimensional polydimethylsiloxane (PDMS) sheet (Fig. 14) [121]. They used a droplet bigger than the volume of the target shape, and then the surplus water is evaporated to form completely closed 3D shapes. Until then, the capillary effect in microfabrication was considered purely detrimental, the one that leads to undesirable stiction in multilayer lithography and coalescence in the case of high aspect ratio structures. The three-dimensional shapes formed using PDMS, however, was temporary. The sheets returned to their original shapes, as soon as the water droplets holding the three-dimensional shape together evaporated. Patterning of the
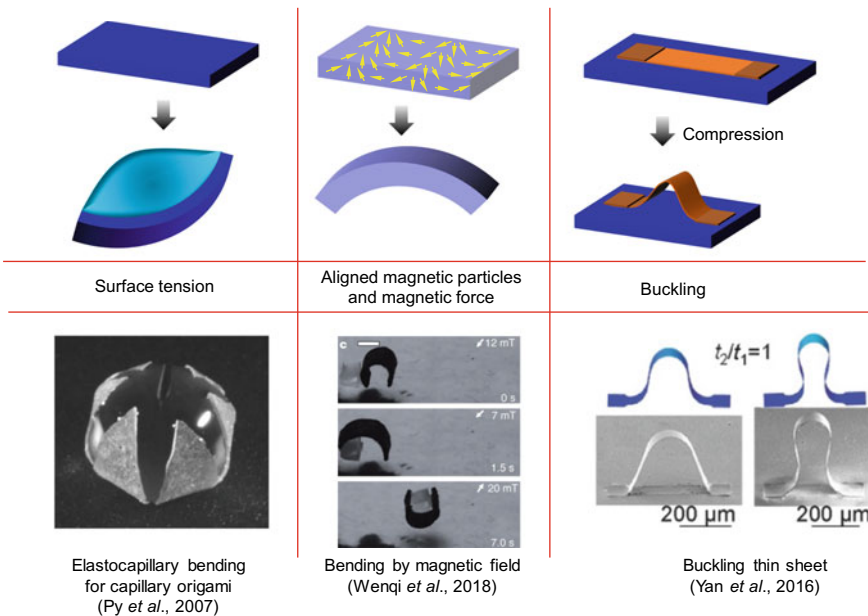
Fig. 14 Implementation of external field approach to obtain *bending* using surface tension [121] (Reproduced with permission, Copyright 2007 by the American Physical Society. https://doi.org/10.1103/PhysRevLett.98.156103), magnetic force [56] (Reproduced by permission from Macmillan Publishers Ltd: Nature, copyright 2018), and compressive force [163] (Copyright 2017 by John Wiley & Sons, Inc. Reproduced by permission of John Wiley & Sons, Inc.)

PDMS sheets to make two-dimensional shapes was challenging too. Moreover, the PDMS sheets had the same material property throughout their planform. Despite these shortcomings, the capillary origami method gave a new facade to one of the lithography limitations and opened a new door to three-dimensional fabrication. High elastic modulus may pose a limitation to this approach when other materials are used. A thinner sheet can be used to overcome the constraints posed by the high elastic modulus values of the materials. For instance, a silicon nitride with a thickness of 100 nm can be bent by the surface tension of water. Another approach to bend a high elastic modulus material is by softening it temporarily, followed by subjecting the material to capillary bending. Polymer sheets, for example, can be softened by heating them above its glass transition temperature.

Magnetic force is exploited for the reversible bending of the elastomers. The fabrication of sheets that can be bent using an external magnet is achieved either using photolithography or using direct writing techniques. The orientation of magnetic particles determines the final folding shape of the sheet. Differently oriented magnetic particles on different faces are initially achieved by orienting the particles inside a curable silicone material using an external magnetic field followed by locking them in place by curing the silicone. A precision of 100 µm is possible with photocurable silicone materials, as shown by Xu et al. [161]. A sinusoidally arranged magnetic particles inside the sheet induce uniform bending on the sheet in a magnetic field, as shown in Fig. 14.

Releasable multilayered 2D precursors are buckled to form complex three-dimensional shapes. These shapes are fabricated using SOI wafers and sacrificial layers. A bonding location is designed, and multiple layers are transferred using polyvinyl alcohol onto a stretched elastomer. When the strain of the elastomer is released, the transferred structure buckles (Fig. 14). Numerous configurations may be formed if the strain releasing sequence is controlled.

3.3.2 From Bending to Folding Using External Field Approach

Capillary-based folding of two-dimensional sheets made of rigid panels and flexible hinges can result in folded three-dimensional shape rather than a bent shape (Fig. 15). The shape obtained represents the configuration corresponding to the energy-optimized state, as explained earlier. (Therefore, the angle to which the sheet folds can be estimated by minimizing both bending and surface energies by assuming that the volume of the droplet placed on the structure remains constant during the folding process [153]). In a negative photoresist, the exposure energy density in a location determines the local degree of crosslinking. The higher the crosslinking density, the stiffer the sheet becomes [36, 43, 44]. Therefore, an origami precursor sheet with stiff faces and compliant folds can be made easily by controlling the exposure. Polymer softens when they are heated to a temperature close to or beyond its glass transition temperature. The softening temperature of a polymer is a function of the degree of crosslinking. As a result, when heated, the precursors soften more at the fold region, leading to folding of the shape upon capillary actuation [43].
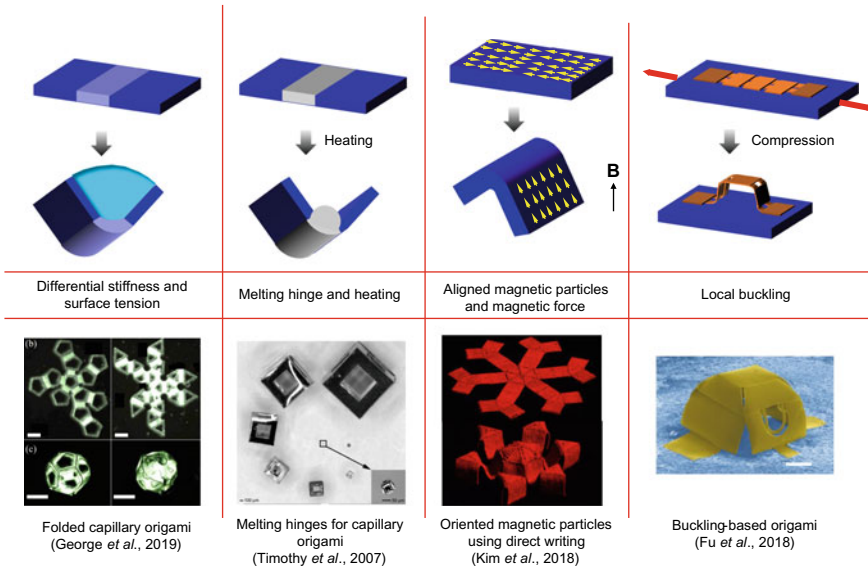
Fig. 15 Implementation of external field approach to obtain *folding* using surface tension [43, 93] (Copyright 2007, American Chemical Society), magnetic force [71] (Reproduced by permission from Macmillan Publishers Ltd: Nature, copyright 2018) and compressive force [40] (Reproduced by permission from Macmillan Publishers Ltd: Nature Materials, copyright 2018)

Multilayer microfabrication technique can be used to make two-dimensional shapes having different materials at different locations, along the length and the thickness. Precursors can be made with high melting point rigid panels and low melting point folds. After releasing from the supporting structure, if these patterned structures are heated, the low melting point materials melt. Consequently, the panels made of high melting point materials is folded because of the surface tension of the melted hinge. Folding by a locally applied solder is an example of such a technique [12, 45]. Photolithography made local deposition of solder possible. This deposition of solder can be combined with other lithography techniques such as e-beam lithography and nanoimprint lithography to make panels with hinges in micro- and nanoscales [79]. These fabrication techniques enable the creation of smaller shapes. Moreover, the absence of any droplets at room temperature makes the fabrication process simpler. However, the materials used in this method are not ideal for most of the biological applications. Implementation of a folding procedure on polymers can overcome this shortcoming [6].

The electrostatic force can drive folding action in millimeter-sized electro-origami robots [141]. Here, the folding is achieved by introducing opposite charges on each face. However, merely applying voltage is not enough to induce folding. The force which drives the folding can be improved dramatically by introducing a liquid droplet having high permittivity and high breakdown strength at the folds. The placement of

liquid bead at the fold region enhances the driving force (Maxwells pressure). Moreover, an application of a high electric field is possible in this technique since the breakdown electric field increases considerably with the introduction of the liquid. Therefore, a high actuation force can be attained here, as compared to a system without any such liquid. This liquid bead prefers to be at the folds due to the electrophoretic forces generated by the high electric field there.

The integration of capillary origami to other existing MEMS components can be realized by patterning conductive materials on top of them. Gold is considered as one of the best options for this application due to its high conductivity and low elastic modulus. The electrical connection between the faces is achieved through the gold connections that are running through the hinges [88]. The low modulus of the gold makes sure that the effect of gold on the folding is minimal. A hand-free bending of the faces is achieved by building conducting loops on them using gold, followed by the application of Lorentz force [129].

As far as the magnetically driven folding is concerned, a sheet where the particle orientation on adjacent faces of the origami is such that they are facing each gives rise to folding in the presence of a uniform magnetic field, as shown in Fig. 15. Aligned magnetic materials are achieved in a polymer matrix through a direct writing technique by sending unaligned magnetizable NdFeB particles through a printer head equipped with aligning magnetic field. In this technique, the aligning magnetic field reorients the particles, and the rheology of the printed material keeps the aligned particle in place. The orientation of the magnetic particles with respect to the printing platform is adjusted by controlling the magnetic field direction and the printing direction.

4   Permanent Folding

A strategy to make a permanently folded structure is to alter the required bending energy temporarily by softening and stiffening the material at relevant instants. A soft material folded with elastocapillary effects if converted into stiff material after the folding can retain the bent shape. This retention is due to the energy-expensive route that it must take to go back to the original flat configuration. One of the ways to achieve this is by exploiting the softening of the polymers. At a lower temperature, the mobility of the molecular chains is low, and this low mobility causes a high stiffness. Polymers, when heated, undergo softening because of the increased mobility of the polymer chains inside the material. The reduced stiffness enables easy folding at an elevated temperature. Subsequent cooling ensures retention of the folded structure. Although such a technique lets the folded structure to keep its shape, it is still not a completely permanent folding method since it can go back to the original shape at an elevated temperature. Chemically altering the polymer could help in overcoming this shortcoming. One way to achieve this change is by controlling the crosslinking of the polymer. The higher the level of crosslinking of a polymer, the higher the stiffness of the material. One of the most explored techniques where crosslinking can be
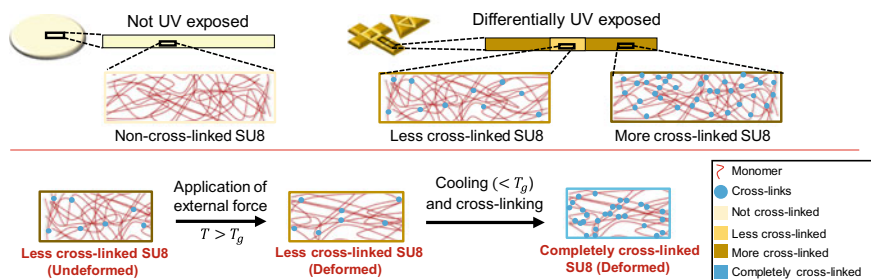
Fig. 16 A strategy to obtain permanently folded shapes using photopolymer [44]. Reprinted with permission from the Royal Society of Chemistry

manipulated with ease is by using a photopolymer. In the case of a negative photoresist that we mentioned earlier in the external field approach section, a partially cross-linked material can be folded at an elevated temperature, brought back to a lower temperature, and then can be completely cross-linked to form a three-dimensional shape which is stable in a wide range of temperature window [44] (Fig. 16).

Folding of two-dimensional sheets that are made of silicon nitride often resulted in permanently closed shapes owing to van der Waals forces, albeit with limited control. Photolithography techniques reduce the surface roughness of the resulting shapes. A sheet pattern with less roughness increases the van der Waals interaction and, therefore, the adhesion. This force can often keep the shape in its folded configuration. However, utilizing this interaction energy alone for making a permanently folded structure in the event of complete evaporation would be unreliable since the gain in energy associated with this may not be always enough to produce repeatable results. Instead of water, if a material that exhibits solid phase at room temperature is used (e.g.,. solder), the folding remains permanent at room temperature. However, the folding has to be performed at an elevated temperature to melt the solder. In one of the early attempts, researchers dipped one whole side of a two-dimensional patterned sheet on melted solder to get enough amount of solder to adhere to that side to drive the folding [45]. The amount of solder transferred to the sheet was critical in achieving the desired target shape. By controlling the surface tension of the liquid and surface energy of the sheet surface, one can control the amount of adhered solder. The energy of the surface can be adjusted with surface treatments such as plasma treatment and chemical cleaning. The surface tension of a liquid, on the other hand, can be altered by changing its temperature. The higher the temperature, the less the surface energy associated with the liquid. These two methods can be utilized to get the right amount of solder on the sheets. Later, researchers lithographically patterned the solder at the folds, allowing for more precise control of the location and quantity of solder.

Although we refrained from mentioning any manual-folding up until now, it would be worth mentioning some such techniques here that form permanently folded shapes. Micro-origami fabrication by Whitesides and group utilized electroplating to join the edges to form permanently folded three-dimensional shapes [16]. Though the folding

of the two-dimensional shapes was performed manually, this welding method has the potential to be extended to smaller dimensions. In a fabrication system, which is a fusion of both direct writing and wet origami technique, origami shapes are obtained by the folding of a directly written layer [2]. The folding is facilitated by the solvent contained in ink, which controls the storage modulus of the structure. The storage modulus increases as the solvent evaporate from the structure. Therefore, a graded volatility solvent system is adopted to have better control over the mechanical properties of the sheets and, thus, a controlled folding [2]. This technique has the capability or makes TiH_2 shape, which later can be converted into TiO_2 by annealing at 1050 °C for 2 h in air. Here patterning is performed by cutting the film, and folding is carried out manually. Another method for making permanently folded shapes is by designing parylene C balloons filled with paraffin wax at the hinges [150]. Wax is melted by sending Joule current to a heater that is fabricated on balloons. The hinges become flexible as a result of this process. The bending is achieved manually, and the heater is turned off to obtain the required rigidity of the folds. The folded shape will go back to the original shape upon reheating. The major drawback of this method is the involvement of complicated fabrication routes and the difficulty associated with injecting wax into the balloons.

5   Carbon Origami MEMS

Carbon microparticles and micropatterns have found various applications, including sensors, flexible electronics, and photonics owing to their unique properties. Surface area, topology, and material properties of carbon influence the design and development of those types of system components. All these qualities can be controlled with the origami design techniques. Releasing of the two-dimensional elements from supporting structures itself increases the available surface area. Folding them and tightly packing them could further increase the available surface area in a unit volume and can create complex topologies that are otherwise difficult to achieve. Carbon also possesses excellent mechanical properties. Shapes like Miura-ori can favorably modify overall mechanical properties even further [101, 134]. However, the carbon materials that we see in day-to-day life are not foldable. That begs the question: how can we make folded carbon shapes?

There are three significant ways to fabricate carbon-based origami.

(1)   By folding graphene or graphene-based materials

Although most of the carbon materials that we are accustomed to are brittle, carbon sheets made of single or multiple layers or atoms—single layer or multilayer graphene—are flexible. Researchers observed sudden changes in the profiles during atomic force microscopy (AFM) scanning of functionalized graphene sheets (FGS). Such changes in the horizontal scan lines indicate the folded FGS resulting from the lateral force exerted by the AFM tip. It proves that the folding of FGS is possible with

an external force. Molecular dynamics simulations show that the folding of graphene using a droplet of liquid is possible too.

A solvent exchange folding is possible with graphene. Graphene-based paper can be designed in such a way that it folds when absorbs water [113]. Fabrication of such a material is performed by locally converting graphene oxide (GO) to GO with polydopamine. When reduced, GO is converted into reduced GO (rGO) that are hydrophobic whereas GO-poly dopamine remains hydrophilic. This difference in the affinity of both materials toward water leads to the local absorption of water to induce reversible bending.

(2)   By integrating carbon onto other materials

Graphene grown by chemical vapor deposition can be transferred onto SU8 by taking advantage of the adhesion force between them [30]. Polyhedral shapes containing graphene are fabricated by combining this transfer with the self-folding of differentially cross-linked SU8 that was explained earlier. This technique offers a new pathway to exploit the attractive qualities of the graphene more effectively. Earlier, we also mentioned about SiO_2-based bimorphs that fold due to residual stress. By including graphene also into that bimorph, a graphene origami can be developed [109].

(3)   By converting folded polymer shape to carbon

Polymers with carbon-rich backbones can be converted into carbon through heat treatment in an inert environment (pyrolysis). During the process, molecules other than carbon are removed, leaving the carbon behind. Interestingly, such a conversion into carbon retains the original polymer shape, but isometrically shrunken. Cellulosic paper survives pyrolysis. So does any forms that are made using cellulosic paper [60]. Therefore, structures made of carbon can be realized by pyrolyzing the paper-based origami. SU8-based polyhedral shapes that are made using capillary origami also can be converted into the corresponding carbon shapes through pyrolysis.

6   Applications of Origami MEMS

Origami at a smaller length scale has various applications in fields including optics, electronics, and biology. The major applications are listed in Table 3.
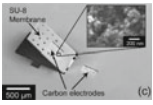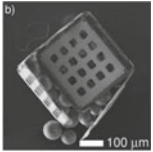
7   Conclusion
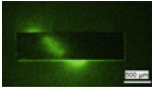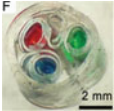
In this chapter, we discussed various strategies for microfabricating origami. Different tactics are generalized as bimorph approach, gradient approach, and

Table 3 Applications of origami

Field	Applications	Representative figures and related references
Optics	Micromirrors	 [169] (Reprinted with the permission of AIP Publishing)
	Three-dimensional optics	 [22] (Copyright 2011 by John Wiley & Sons, Inc. Reproduced by permission of John Wiley & Sons, Inc.)
	Stages	[76]
Electrical and electronic	Three-dimensional electronics	 [122] (Reprinted with the permission of AIP Publishing) [46, 50, 72, 73, 172]
	Flexible electronics	 [111] (Reproduced with permission. © IOP Publishing. All rights reserved)
	Self-folding and self-degrading robots	 [159] (Reproduced with permission. © IOP Publishing. All rights reserved) [110, 116]
	Solar panels	 [82] [108, 143]
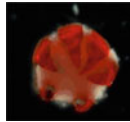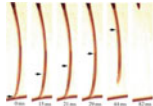
Table 3 (continued)

Field	Applications	Representative figures and related references
	Energy storage	 [58] (Reprinted with the permission of AIP Publishing) [135]
Biomedical	Encapsulation	 [95] (Reprinted with permission from the Royal Society of Chemistry) [48, 92, 94]
	Drug delivery	 [67] (Copyright 2011 by John Wiley & Sons, Inc. Reproduced by permission of John Wiley & Sons, Inc.) [37]
	Microtube fabrication	 [66] (Copyright 2013 by John Wiley & Sons, Inc. Reproduced by permission of John Wiley & Sons, Inc.) [19, 57, 64]
	Scaffold for tissue engineering	 [61] (Copyright 2010, reprinted with permission from Elsevier) [62, 68]

Table 3 (continued)

Field	Applications	Representative figures and related references
	Micro-grippers	 [104] (Copyright 2014 by John Wiley & Sons, Inc. Reproduced by permission of John Wiley & Sons, Inc.) [94]
	Stent to open blocked arteries	 [78] (Copyright 2010, reprinted with permission from Elsevier)
In nature	Leaves	[103]
	Hummingbird's tongue	 [70] (Reprinted with permission from the Royal Society, U. K.) [125]
	Mimosa	[155]
	Insect wing	[34]
	Seed pod	[4, 39]

external field approach. The folding methods explained in this chapter in conjunction with bottom-up methods such as DNA origami are hoped to span the entire submillimeter range. While there are numerous fabrication approaches for achieving folding at submillimeter scale, process of making positive and negative Gaussian curvatures within a single shape, curved folds (curved origami), and sequentially folding folds at this scale are remaining as paths less traveled. Despite having these less explored fabrication regimes, origami finds applications as micro-containers, micro-grippers, cell encapsulating device, 3D electronics platform, tissue scaffold, and many more. It is these applications that fueled the rapid growth of the origami MEMS technology in the last decade. Origami will continue to benefit electronics, photonics, energy sector, and biomedical field, if the fabrication routes are simplified, and are made more reliable. Considering that the design of origami MEMS can be inspired by other matured fields including macroscale origami, and compliant mechanism, we expect the growth in this field to sustain its pace. The development of design platforms and modeling software should follow the ongoing origami research to achieve these goals of making it simpler and more reliable, and thus to open itself

to a broader audience. It should also be noted that the future of the origami MEMS is not just confined to three-dimensional shapes that it can form, rather the dynamics of the folding process and the effect the folding can have on the material properties will also be of importance. The dynamics of the folding process has already been investigated a little in the 4D printing methods that were mentioned earlier in the chapter. Such transformable structures could form reconfigurable shapes and meta-materials. Folding realized by various techniques discussed in this chapter can have different effects on the obtained origami structure and/or the material. Those side-effects are yet to be studied in detail. Such exploration is imperative to develop reliable and affordable, high-resolution multi-functional origami fabrication techniques.

References

1. Agrawal, A., Yun, T., Pesek, S.L., et al.: Shape-responsive liquid crystal elastomer bilayers. Soft Matter **10**, 1411–1415 (2014). https://doi.org/10.1039/c3sm51654g
2. Ahn, B.Y., Shoji, D., Hansen, C.J., et al.: Printed origami structures. Adv. Mater. **22**, 2251–2254 (2010). https://doi.org/10.1002/adma.200904232
3. Andres, C.M., Zhu, J., Shyu, T., et al.: Shape-morphing nanocomposite origami. Langmuir **30**, 5378–5385 (2014). https://doi.org/10.1021/la404955s
4. Armon, S., Efrati, E., Kupferman, R., Sharon, E.: Geometry and mechanics in the opening of chiral seed pods. Science (80-) **297**, 5–9 (2002)
5. Arora, W.J., Nichol, A.J., Smith, H.I., Barbastathis, G.: Membrane folding to achieve three-dimensional nanostructures: nanopatterned silicon nitride folded with stressed chromium hinges. Appl. Phys. Lett. **88**, 1–3 (2006). https://doi.org/10.1063/1.2168516
6. Azam, A., Laflin, K.E., Jamal, M., et al.: Self-folding micropatterned polymeric containers. Biomed. Microdevices **13**, 51–58 (2011). https://doi.org/10.1007/s10544-010-9470-x
7. Bassik, N., Abebe, B.T., Laflin, K.E., Gracias, D.H.: Photolithographically patterned smart hydrogel based bilayer actuators. Polymer (Guildf) **51**, 6093–6098 (2010). https://doi.org/10.1016/j.polymer.2010.10.035
8. Bassik, N., Brafman, A., Zarafshar, A.M., et al.: Enzymatically triggered actuation of minia-turized tools. J. Am. Chem. Soc. **132**, 16314–16317 (2010). https://doi.org/10.1021/ja106218s
9. Bassik, N., Stern, G.M., Gracias, D.H.: Microassembly based on hands free origami with bidirectional curvature. Appl. Phys. Lett. **95**, 1–4 (2009). https://doi.org/10.1063/1.3212896
10. Behl, M., Kratz, K., Zotzmann, J., et al.: Reversible bidirectional shape-memory polymers. Adv. Mater. **25**, 4466–4469 (2013). https://doi.org/10.1002/adma.201300880
11. Behl, M., Razzaq, M.Y., Lendlein, A.: Multifunctional shape-memory polymers. Adv. Mater. **22**, 3388–3410 (2010). https://doi.org/10.1002/adma.200904447
12. Boncheva, M., Bruzewicz, D.A., Whitesides, G.M.: Millimeter-scale self-assembly and its applications. Pure Appl. Chem. **75**, 621–630 (2003). https://doi.org/10.1351/pac200375050621
13. Boncheva, M., Whitesides, G.M.: Templated self-assembly: Formation of folded structures by relaxation of pre-stressed, planar tapes. Adv. Mater. **17**, 553–557 (2005). https://doi.org/10.1002/adma.200400940
14. Boothby, J.M., Ware, T.H.: Dual-responsive, shape-switching bilayers enabled by liquid crystal elastomers. Soft Matter **13**, 4349–4356 (2017). https://doi.org/10.1039/c7sm00541e
15. Boyvat, M., Koh, J.S., Wood, R.J.: Addressable wireless actuation for multijoint folding robots and devices. Sci. Robot. **2**, 1–10 (2017). https://doi.org/10.1126/scirobotics.aan1544

16. Brittain, S.T., Schueller, O.J.A., Wu, H.K., et al.: Microorigami: fabrication of small, three-dimensional, metallic structures. J. Phys. Chem. B **105**, 347–350 (2001). https://doi.org/10.1021/Jp002556e

17. Byun, M., Santangelo, C.D., Hayward, R.C.: Swelling-driven rolling and anisotropic expansion of striped gel sheets. Soft Matter **9**, 8264–8273 (2013). https://doi.org/10.1039/c3sm50627d

18. Chen, D., Yoon, J., Chandra, D., et al.: Stimuli-responsive buckling mechanics of polymer films. J. Polym. Sci. Part B Polym. Phys. **52**, 1441–1461 (2014). https://doi.org/10.1002/polb.23590

19. Chia Gómez, L.P., Bollgruen, P., Egunov, A.I., et al.: Vapour processed self-rolled poly(dimethylsiloxane) microcapillaries form microfluidic devices with engineered inner surface. Lab Chip **13**, 3827–3831 (2013). https://doi.org/10.1039/c3lc50542a

20. Cho, J., Gracias, D.H.: Self-assembly of lithographically patterned nanoparticles. Nano Lett. **9**, 4048–4051 (2009)

21. Cho, J.H., James, T., Gracias, D.H.: Curving nanostructures using extrinsic stress. Adv. Mater. **22**, 2320–2324 (2010). https://doi.org/10.1002/adma.200904410

22. Cho, J.H., Keung, M.D., Verellen, N., et al.: Nanoscale origami for 3D optics. Small **7**, 1943–1948 (2011). https://doi.org/10.1002/smll.201100568

23. Chua, C.L., Fork, D.K., Van, S.K., Lu, J.: Out-of-plane high-Q inductors on low-resistance silicon. J. Microelectromech. Syst. **12**, 989–995 (2003)

24. Cisquella-Serra, A., Magnani, M., Gual-Mosegui, Á., et al.: Study of the electrostatic jet initiation in near-field electrospinning. J. Colloid Interface Sci. **543**, 106–113 (2019). https://doi.org/10.1016/j.jcis.2019.02.041

25. Cui, J., Huang, T.Y., Luo, Z., et al.: Nanomagnetic encoding of shape-morphing micromachines. Nature **575**, 164–168 (2019). https://doi.org/10.1038/s41586-019-1713-2

26. Davis, D., Mailen, R., Genzer, J., Dickey, M.D.: Self-folding of polymer sheets using microwaves and graphene ink. RSC Adv. **5**, 89254–89261 (2015). https://doi.org/10.1039/c5ra16431a

27. Dawson, C., Vincent, J.F.V., Rocca, A.M.: How pine cones open. Nature **390**, 668 (1997). https://doi.org/10.1038/37745

28. De Haan, L.T., Sánchez-Somolinos, C., Bastiaansen, C.M.W., et al.: Engineering of complex order and the macroscopic deformation of liquid crystal polymer networks. Angew. Chem. Int. Ed. **51**, 12469–12472 (2012). https://doi.org/10.1002/anie.201205964

29. Demaine, E.D., Tachi, T.: Origamizer: a practical algorithm for folding any polyhedron. Leibniz Int. Proc. Inform. LIPIcs **77**, 341–3416 (2017). https://doi.org/10.4230/LIPIcs.SoCG.2017.34

30. Deng, T., Yoon, C., Jin, Q., et al.: Self-folding graphene-polymer bilayers. Appl. Phys. Lett. **106** (2015). https://doi.org/10.1063/1.4921530

31. Ding, Z., Yuan, C., Peng, X., et al.: Direct 4D printing via active composite materials. Sci. Adv. **3** (2017). https://doi.org/10.1126/sciadv.1602890

32. Dunn, M.L., Zhang, Y., Bright, V.M.: Deformation and structural stability of layered plate microstructures subjected to thermal loading. J. Microelectromech. Syst. **11**, 372–384 (2002). https://doi.org/10.1109/JMEMS.2002.800932

33. Eder, F., Klauk, H., Halik, M., et al.: Organic electronics on paper. Appl. Phys. Lett. **84**, 2673–2675 (2004). https://doi.org/10.1063/1.1690870

34. Faber, J.A., Arrieta, A.F., Studart, A.R.: Bioinspired spring origami. Science (80-) **359**, 1386–1391 (2018). https://doi.org/10.1126/science.aap7753

35. Felton, S.M., Becker, K.P., Aukes, D.M., Wood, R.J.: Self-folding with shape memory composites at the millimeter scale. J. Micromech. Microeng. **25** (2015). https://doi.org/10.1088/0960-1317/25/8/085004

36. Feng, R., Farris, R.J.: Influence of processing conditions on the thermal and mechanical properties of SU8 negative photoresist coatings. J. Micromech. Microeng. **13**, 80–88 (2003)

37. Fernandes, R., Gracias, D.H.: Self-folding polymeric containers for encapsulation and delivery of drugs. Adv. Drug Deliv. Rev. **64**, 1579–1589 (2012). https://doi.org/10.1016/j.addr.2012.02.012

38. Filipiak, D.J., Azam, A., Leong, T.G.: Hierarchical self-assembly of complex polyhedral microcontainers. J. Micromech. Microeng. **075012**, 1–6 (2009). https://doi.org/10.1088/0960-1317/19/7/075012

39. Forterre, Y., Dumais, J.: Generating helices in nature **333**, 1715–1717 (2011)

40. Fu, H., Nan, K., Bai, W., et al.: Morphable 3D mesostructures and microelectronic devices by multistable buckling mechanics. Nat. Mater. **17**, 268–276 (2018). https://doi.org/10.1038/s41563-017-0011-3

41. Ge, Q., Dunn, C.K., Qi, H.J., Dunn, M.L.: Active origami by 4D printing. Smart Mater. Struct. **23** (2014). https://doi.org/10.1088/0964-1726/23/9/094007

42. Ge, Q., Qi, H.J., Dunn, M.L.: Active materials by four-dimension printing. Appl. Phys. Lett. **103** (2013). https://doi.org/10.1063/1.4819837

43. George, D., Hernandez, E.A.P., Madou, M.: Origami fabrication using single layer photolithography and capillary folding. In: Proceedings of the 7th International Workshop on Nanotechnology and its Applications (2019a)

44. George, D., Madou, M., Hernandez, E.A.P, Lo, R.C.: Fabrication of polymer and carbon polyhedra through controlled cross-linking and capillary deformations 9171–9177 (2019b). https://doi.org/10.1039/c9sm01410a

45. Gracias, D.H., Kavthekar, V., Love, J.C., et al.: Fabrication of micrometer-scale, patterned polyhedra by self-assembly. Adv. Mater. **14**, 235–238 (2002). https://doi.org/10.1002/1521-4095(20020205)14:3%3c235:AID-ADMA235%3e3.0.CO;2-B

46. Gracias, D.H., Tien, J., Breen, T.L., et al.: Forming electrical networks in three dimensions by self-assembly. Science (80-) **289**, 1170–1172 (2000). https://doi.org/10.1126/science.289.5482.1170

47. Guan, J., He, H., Hansford, D.J., Lee, L.J.: Self-folding of three-dimensional hydrogel microstructures. J. Phys. Chem. B **109**, 23134–23137 (2005). https://doi.org/10.1021/jp054341g

48. Gultepe, E., Randhawa, J.S., Kadam, S., et al.: Biopsy with thermally-responsive untethered microtools. Adv. Mater. **25**, 514–519 (2013). https://doi.org/10.1002/adma.201203348

49. Guo, L., Anderson, D.G., Langer, R.: Bio-Inspired polymer composite actuator and generator driven by water gradients. Science (80-) **339**, 9–12 (2012)

50. Guo, X., Li, H., Yeop Ahn, B., et al.: Two- and three-dimensional folding of thin film single-crystalline silicon for photovoltaic power applications. Proc. Natl. Acad. Sci. **106**, 20149–20154 (2009). https://doi.org/10.1073/pnas.0907390106

51. Hauser, A.W., Evans, A.A., Na, J.H., Hayward, R.C.: Photothermally reprogrammable buckling of nanocomposite gel sheets. Angew. Chem. Int. Ed. **54**, 5434–5437 (2015). https://doi.org/10.1002/anie.201412160

52. Holmes, D.P., Roché, M., Sinha, T., Stone, H.A.: Bending and twisting of soft materials by non-homogenous swelling. Soft Matter **7**, 5188–5193 (2011). https://doi.org/10.1039/c0sm01492c

53. Hong, F., Zhang, F., Liu, Y., Yan, H.: DNA Origami: Scaffolds for Creating Higher Order Structures (2017)

54. Hu, G.F., Damanpack, A.R., Bodaghi, M., Liao, W.H.: (2017) Increasing dimension of structures by 4D printing shape memory polymers via fused deposition modeling. Smart Mater. Struct. **26**. https://doi.org/10.1088/1361-665X/aa95ec

55. Hu, L., Choi, J.W., Yang, Y., et al.: Highly conductive paper for energy-storage devices. Proc. Natl. Acad. Sci. U.S.A. **106**, 21490–21494 (2009). https://doi.org/10.1073/pnas.0908858106

56. Hu, W., Lum, G.Z., Mastrangeli, M., Sitti, M.: Small-scale soft-bodied robot with multimodal locomotion. Nature **554**, 81–85 (2018). https://doi.org/10.1038/nature25443

57. Huang, W., Koric, S., Yu, X., et al.: Precision structural engineering of self-rolled-up 3D nanomembranes guided by transient quasi-static FEM modeling. Nano Lett. **14**, 6293–6297 (2014). https://doi.org/10.1021/nl5026369

58. In, H.J., Kumar, S., Shao-Horn, Y., Barbastathis, G.: Origami fabrication of nanostructured, three-dimensional devices: electrochemical capacitors with carbon electrodes. Appl. Phys. Lett. **88**, 6–9 (2006). https://doi.org/10.1063/1.2177639

59. Ionov, L.: Soft microorigami: self-folding polymer films. Soft Matter **7**, 6786–6791 (2011). https://doi.org/10.1039/c1sm05476g

60. Islam, M., Flach, J., Martinez-Duarte, R.: Carbon origami: a method to fabricate lightweight carbon cellular materials. Carbon N Y **133**, 140–149 (2018). https://doi.org/10.1016/j.carbon.2018.03.033

61. Jamal, M., Bassik, N., Cho, J.H., et al.: Directed growth of fibroblasts into three dimensional micropatterned geometries via self-assembling scaffolds. Biomaterials **31**, 1683–1690 (2010). https://doi.org/10.1016/j.biomaterials.2009.11.056

62. Jamal, M., Kadam, S.S., Xiao, R., et al.: Bio-origami hydrogel scaffolds composed of photocrosslinked PEG bilayers. Adv. Healthc. Mater. **2**, 1142–1150 (2013). https://doi.org/10.1002/adhm.201200458

63. Jamal, M., Zarafshar, A.M., Gracias, D.H.: Differentially photo-crosslinked polymers enable self-assembling microfluidics. Nat. Commun. **2**, 526–527 (2011). https://doi.org/10.1038/ncomms1531

64. Jamal, M., Zarafshar, A.M., Gracias, D.H.: Differentially photo-crosslinked polymers enable self-assembling microfluidics. Nat. Commun. **2**, 527 (2013). https://doi.org/10.1038/ncomms1531.Differentially

65. Janbaz, S., Hedayati, R., Zadpoor, A.A.: Programming the shape-shifting of flat soft matter: from self-rolling/self-twisting materials to self-folding origami. Mater. Horiz. **3**, 536–547 (2016). https://doi.org/10.1039/c6mh00195e

66. Jin, Y., Wang, N., Yuan, B., et al.: Stress-induced self-assembly of complex three dimensional structures by elastic membranes. Small **9**, 2410–2414 (2013). https://doi.org/10.1002/smll.201300929

67. Kalinin, Y.V., Randhawa, J.S., Gracias, D.H.: Three-dimensional chemical patterns for cellular self-organization. Angew. Chem. Int. Ed. **50**, 2549–2553 (2011). https://doi.org/10.1002/anie.201007107

68. Kempaiah, R., Nie, Z.: From nature to synthetic systems: Shape transformation in soft materials. J. Mater. Chem. B **2**, 2357–2368 (2014). https://doi.org/10.1039/c3tb21462a

69. Kim, J., Hanna, J.A., Hayward, R.C., Santangelo, C.D.: Thermally responsive rolling of thin gel strips with discrete variations in swelling. Soft Matter **8**, 2375–2381 (2012). https://doi.org/10.1039/c2sm06681e

70. Kim, W., Peaudecerf, F., Baldwin, M.W., Bush, J.W.M.: The hummingbird's tongue: a self-assembling capillary syphon. Proc. R. Soc. B Biol. Sci. **279**, 4990–4996 (2012). https://doi.org/10.1098/rspb.2012.1837

71. Kim, Y., Yuk, H., Zhao, R., et al.: Printing ferromagnetic domains for untethered fast-transforming soft materials. Nature **558**, 274 (2018). https://doi.org/10.1038/s41586-018-0185-0

72. Kimionis, J., Georgiadis, A., Isakov, M., et al.: 3D/inkjet-printed origami antennas for multi-direction RF harvesting. In: 2015 IEEE MTT-S International Microwave Symposium, IMS 2015, pp.1–4 (2015a). https://doi.org/10.1109/MWSYM.2015.7166878

73. Kimionis, J., Isakov, M., Koh, B.S., et al.: 3D-printed origami packaging with inkjet-printed antennas for RF harvesting sensors. IEEE Trans. Microw. Theory Tech. **63**, 4521–4532 (2015). https://doi.org/10.1109/TMTT.2015.2494580

74. Kobayashi, K., Oh, S.H., Yoon, C., Gracias, D.H.: Multitemperature responsive self-folding soft biomimetic structures. Macromol. Rapid Commun. **1700692**, 1–7 (2018). https://doi.org/10.1002/marc.201700692

75. Konotop, I.Y., Nasimova, I.R., Tamm, M.V., et al.: Novel pH-responsive hydrogels with gradient charge distribution. Soft Matter **6**, 1632–1634 (2010). https://doi.org/10.1039/b923804b

76. Kubota, K., Fleischmann, T., Saravanan, S., et al.: Self-assembly of micro-stage using micro-origami technique on GaAs. In: 2002 International Microprocesses and Nanotechnology Conference, MNC 2002, p. 326 (2002). https://doi.org/10.1109/IMNC.2002.1178675

77. Kuribayashi-Shigetomi, K., Onoe, H., Takeuchi, S.: Cell Origami: Self-folding of three-dimensional cell-laden microstructures driven by cell traction force. PLoS One **7**, 1–8 (2012). https://doi.org/10.1371/journal.pone.0051085

78. Kuribayashi, K., Tsuchiya, K., You, Z., et al.: Self-deployable origami stent grafts as a biomedical application of Ni-rich TiNi shape memory alloy foil. Mater. Sci. Eng. A **419**, 131–137 (2006). https://doi.org/10.1016/j.msea.2005.12.016

79. Kwag, H.R., Cho, J.-H., Park, S.-Y., et al.: Self-folding nanostructures with imprint patterned surfaces (SNIPS). Faraday Discuss. **191**, 61–71 (2016). https://doi.org/10.1039/c6fd00021e

80. Laflin, K.E., Morris, C.J., Muqeem, T., Gracias, D.H.: Laser triggered sequential folding of microstructures. Appl. Phys. Lett. **101** (2012). https://doi.org/10.1063/1.4754607

81. Lahikainen, M., Zeng, H., Priimagi, A.: Reconfigurable photoactuator through synergistic use of photochemical and photothermal effects. Nat. Commun. **9**, 1–8 (2018). https://doi.org/10.1038/s41467-018-06647-7

82. Lamoureux, A., Lee, K., Shlian, M., et al.: Dynamic kirigami structures for integrated solar tracking. Nat. Commun. **6**, 1–6 (2015). https://doi.org/10.1038/ncomms9092

83. Lamprecht, B., Thünauer, R., Ostermann, M., et al.: Organic photodiodes on newspaper. Phys. Status Solidi Appl. Mater. Sci. **202**, 50–52 (2005). https://doi.org/10.1002/pssa.200510010

84. Lauff, C., Simpson, T.W., Frecker, M., et al.: Differentiating bending from folding in origami engineering using active materials. In: International Design Engineering Technical Conferences & Computers and Information in Engineering Conference, pp 1–12 (2014)

85. Lee, B.P., Konst, S.: Novel hydrogel actuator inspired by reversible mussel adhesive protein chemistry. Adv. Mater. **26**, 3415–3419 (2014). https://doi.org/10.1002/adma.201306137

86. Lee, D.W., Phadikar, J., Shankar, M.R.: Multiplicity of shape selection in functionally graded liquid crystalline polymers. RSC Adv. **7**, 23046–23054 (2017). https://doi.org/10.1039/c7ra03465b

87. Lee, K.M., Smith, M.L., Koerner, H., et al.: Photodriven, flexural-torsional oscillation of glassy azobenzene liquid crystal polymer networks. Adv. Funct. Mater. **21**, 2913–2918 (2011). https://doi.org/10.1002/adfm.201100333

88. Legrain, A., Berenschot, J.W., Tas, N.R., Abelmann, L.: Capillary origami of micro-machined micro-objects: Bi-layer conductive hinges. Microelectron. Eng. **140**, 60–66 (2015). https://doi.org/10.1016/j.mee.2015.06.004

89. Lendlein, A., Gould, O.E.C.: Reprogrammable recovery and actuation behaviour of shape-memory polymers. Nat. Rev. Mater. **4**, 116–133 (2019). https://doi.org/10.1038/s41578-018-0078-8

90. Lendlein, A., Jiang, H., Junger, O., Langer, R.: Light-induced shape-memory polymers. Nature **434**, 695–697 (2005). https://doi.org/10.1038/nature03438.1

91. Lendlein, A., Shastri, V.P.: Stimuli-sensitive polymers. Adv. Mater. **22**, 3344–3347 (2010). https://doi.org/10.1002/adma.201002520

92. Leong, T.G., Benson, B.R., Call, E.K., Gracias, D.H.: Thin film stress driven self-folding of microstructured containers. Small **4**, 1605–1609 (2008). https://doi.org/10.1002/smll.200800280

93. Leong, T.G., Lester, P.A., Koh, T.L., et al.: Surface tension-driven self-folding polyhedra. Langmuir **23**, 8747–8751 (2007). https://doi.org/10.1021/la700913m

94. Leong, T.G., Randall, C.L., Benson, B.R., et al.: Tetherless thermobiochemically actuated microgrippers. Proc. Natl. Acad. Sci. U.S.A. **106**, 703–708 (2009). https://doi.org/10.1073/pnas.0807698106

95. Leong, T.G., Randall, C.L., Benson, B.R., et al.: Self-loading lithographically structured microcontainers: 3D patterned, mobile microwells. Lab Chip **8**, 1621–1624 (2008). https://doi.org/10.1039/b809098j

96. Liu, F., Urban, M.W.: Recent advances and challenges in designing stimuli-responsive polymers. Prog. Polym. Sci. **35**, 3–23 (2010). https://doi.org/10.1016/j.progpolymsci.2009.10.002

97. Liu, Y., Boyles, J.K., Genzer, J., Dickey, M.D.: Self-folding of polymer sheets using local light absorption. Soft Matter **8**, 1764–1769 (2012). https://doi.org/10.1039/c1sm06564e

98. Liu, Y., Miskiewicz, M., Escuti, M.J., et al.: Three-dimensional folding of pre-strained polymer sheets via absorption of laser light. J. Appl. Phys. **115** (2014). https://doi.org/10.1063/1.4880160

99. Lu, X., Zhang, H., Fei, G., et al.: Liquid-crystalline dynamic networks doped with gold nanorods showing enhanced photocontrol of actuation. Adv. Mater. **30**, 1–8 (2018). https://doi.org/10.1002/adma.201706597

100. Luo, C.J., Stoyanov, S.D., Stride, E., et al.: Electrospinning versus fibre production methods: from specifics to technological convergence. Chem. Soc. Rev. **41**, 4708 (2012). https://doi.org/10.1039/c2cs35083a

101. Lv, C., Krishnaraju, D., Konjevod, G., et al.: Origami based mechanical metamaterials. Sci. Rep. **4** (2014). https://doi.org/10.1038/srep05979

102. Madou, M.J.: Fundamentals of Microfabrication and Nanotechnology-Volume II (2011)

103. Mahadevan, L., Rica, S.: Self-organized origami. Science (80-) **307**, 1740 (2005). https://doi.org/10.1126/science.1105169

104. Malachowski, K., Breger, J., Kwag, H.R., et al.: Stimuli-responsive theragrippers for chemo-mechanical controlled release. Angew. Chem. Int. Ed. **53**, 8045–8049 (2014). https://doi.org/10.1002/anie.201311047

105. Manakasettharn, S., Ashley Taylor, J., Krupenkin, T.N.: Bio-inspired artificial iridophores based on capillary origami: fabrication and device characterization. Appl. Phys. Lett. **99**, 2012–2015 (2011). https://doi.org/10.1063/1.3646394

106. Mao, Y., Yu, K., Isakov, M.S., et al.: Sequential self-folding structures by 3D printed digital shape memory polymers. Sci. Rep. **13616**, 1–12 (2015). https://doi.org/10.1038/srep13616

107. Martinez, A.W., Phillips, S.T., Butte, M.J., Whitesides, G.M.: Patterned paper as a platform for inexpensive, low-volume, portable bioassays. Angew. Chem. Int. Ed. **46**, 1318–1320 (2007). https://doi.org/10.1002/anie.200603817

108. Mikulas, M.M., Pappa, R.S., Warren, .J, Rose, G.: Telescoping Solar Array Concept for Achieving High Packaging Efficiency. In: 2nd AIAA SciTech Forum, pp. 1–21 (2015). https://doi.org/10.2514/6.2015-1398

109. Miskin, M.Z., Dorsey, K.J., Bircan, B., et al.: Graphene-based bimorphs for micron-sized, tautonomous origami machines. Proc. Natl. Acad. Sci. U.S.A. **115**, 466–470 (2018). https://doi.org/10.1073/pnas.1712889115

110. Miyashita, S., Guitron, S., Ludersdorfer, M., et al.: An untethered miniature origami robot that self-folds, walks, swims, and degrades. In: Proceedings of the IEEE International Conference on Robotics and Automation, pp. 1490–1496 (2015). https://doi.org/10.1109/ICRA.2015.7139386

111. Miyashita, S., Meeker, L., Tolley, M.T., et al.: Self-folding miniature elastic electric devices. Smart Mater. Struct. **23** (2014). https://doi.org/10.1088/0964-1726/23/9/094005

112. Moiseeva, E., Senousy, Y.M., McNamara, S., Harnett, C.K.: Single-mask microfabrication of three-dimensional objects from strained bimorphs. J Micromech. Microeng. **17** (2007). https://doi.org/10.1088/0960-1317/17/9/N01

113. Mu, J., Hou, C., Wang, H., et al.: Origami-inspired active graphene-based paper for programmable instant self-folding walking devices. Sci. Adv. **1**, 1–9 (2015). https://doi.org/10.1126/sciadv.1500533

114. Na, J.H., Evans, A.A., Bae, J., et al.: Programming reversibly self-folding origami with micropatterned photo-crosslinkable polymer trilayers. Adv. Mater. **27**, 79–85 (2015). https://doi.org/10.1002/adma.201403510

115. Ohm, C., Brehmer, M., Zentel, R.: Liquid crystalline elastomers as actuators and sensors. Adv. Mater. **22**, 3366–3387 (2010). https://doi.org/10.1002/adma.200904059

116. Paik, J.K., Kramer, R.K., Wood, R.J.: Stretchable circuits and sensors for robotic origami. In: IEEE International Conference on Intelligent Robots and Systems, pp. 414–420 (2011). https://doi.org/10.1109/IROS.2011.6048353

117. Pandey, S., Ewing, M., Kunas, A., et al.: Algorithmic design of self-folding polyhedra. Proc. Natl. Acad. Sci. **108**, 19885–19890 (2011). https://doi.org/10.1073/pnas.1110857108

118. Peraza-Hernandez, E.A., Hartl, D.J., Malak, R.J., Lagoudas, D.C.: Origami-inspired active structures: a synthesis and review. Smart Mater. Struct. **23** (2014). https://doi.org/10.1088/0964-1726/23/9/094001

119. Piñeirua, M., Bico, J., Roman, B.: Capillary origami controlled by an electric field. Soft Matter **6**, 4491 (2010). https://doi.org/10.1039/c0sm00004c

120. Piqué, A., Mathews, S.A., Charipar, N.A., Birnbaum, A.J.: Laser origami: a new technique for assembling 3D microstructures. In: Laser-Based Micro- and Nanopackaging and Assembly VI, vol. 8244, p. 82440B (2012). https://doi.org/10.1117/12.909187

121. Py, C., Reverdy, P., Doppler, L., et al.: Capillary origami: spontaneous wrapping of a droplet with an elastic sheet. Phys. Rev. Lett. **98**, 2–5 (2007). https://doi.org/10.1103/PhysRevLett.98.156103

122. Randhawa, J.S., Gurbani, S.S., Keung, M.D., et al.: Three-dimensional surface current loops in terahertz responsive microarrays. Appl. Phys. Lett. **96**, 1–4 (2010). https://doi.org/10.1063/1.3428657

123. Rath, A., Mathesan, S., Ghosh, P.: Folding behavior and molecular mechanism of cross-linked biopolymer film in response to water. Soft Matter **12**, 9210–9222 (2016). https://doi.org/10.1039/C6SM01994C

124. Ratna, D., Karger-Kocsis, J.: Recent advances in shape memory polymers and composites: a review. J. Mater. Sci. **43**, 254–269 (2008). https://doi.org/10.1007/s10853-007-2176-7

125. Rico-guevara, A., Rubega, M.A.: The hummingbird tongue is a fluid trap, not a capillary tube (2011) **108**, 1–5. https://doi.org/10.1073/pnas.1016944108

126. Lang, R.J.: Origami Design Secrets: Mathematical Methods for an Ancient Art (2011)

127. Rojas, J.P., Conchouso, D., Arevalo, A., et al.: Paper-based origami flexible and foldable thermoelectric nanogenerator. Nano Energy **31**, 296–301 (2017). https://doi.org/10.1016/j.nanoen.2016.11.012

128. Ryu, J., D'Amato, M., Cui, X., et al.: Photo-origami-bending and folding polymers with light. Appl. Phys. Lett. **100** (2012). https://doi.org/10.1063/1.3700719

129. Shaar, N.S., Barbastathis, G., Livermore, C.: Integrated folding, alignment, and latching for reconfigurable origami microelectromechanical systems. J. Microelectromech. Syst. **24**, 1043–1051 (2015). https://doi.org/10.1109/JMEMS.2014.2379432

130. Shankland, K., Mccusker, L.B., Palatinus, L., et al.: Shaping of elastic sheets by prescription of non-Euclidean metrics. Science **9**, 1116–1120 (2007). https://doi.org/10.1126/science.1137920

131. Shigemune, H., Maeda, S., Hara, Y., et al.: Origami robot: a self-folding paper robot with an electrothermal actuator created by printing. IEEE/ASME Trans. Mechatron. **21**, 2746–2754 (2016). https://doi.org/10.1109/TMECH.2016.2593912

132. Shim, T.S., Kim, S.H., Heo, C.J., et al.: Controlled origami folding of hydrogel bilayers with sustained reversibility for robust microcarriers. Angew. Chem. Int. Ed. **51**, 1420–1423 (2012). https://doi.org/10.1002/anie.201106723

133. Si, K.J., Sikdar, D., Chen, Y., et al.: Giant plasmene nanosheets, nanoribbons, and origami. ACS Nano **8**, 11086–11093 (2014).

134. Silverberg J.L., Evans, A.A., McLeod, L., et al.: Using origami design principles to fold reprogrammable mechanical metamaterials. Science (80-) **345**, 647–650 (2014)

135. Song, Z., Ma, T., Tang, R., et al.: Origami lithium-ion batteries. Nat. Commun. **5** (2014). https://doi.org/10.1038/ncomms4140

136. Stoychev, G., Puretskiy, N., Ionov, L.: Self-folding all-polymer thermoresponsive microcapsules. Soft Matter **7**, 3277–3279 (2011). https://doi.org/10.1039/c1sm05109a

137. Stoychev, G., Turcaud, S., Dunlop, J.W.C., Ionov, L.: Hierarchical multi-step folding of polymer bilayers. Adv. Funct. Mater. **23**, 2295–2300 (2013). https://doi.org/10.1002/adfm.201203245

138. Stoychev, G., Zakharchenko, S., Turcaud, S., et al.: Shape-programmed folding of stimuli-responsive polymer bilayers. ACS Nano **6**, 3925–3934 (2012). https://doi.org/10.1021/nn300079f

139. Sun, Y., Choi, W.M., Jiang, H., et al.: Controlled buckling of semiconductor nanoribbons for stretchable electronics. Nat. Nanotechnol. **1**, 201–207 (2006). https://doi.org/10.1038/nnano.2006.131

140. Sydney Gladman, A., Matsumoto, E.A., Nuzzo, R.G., et al.: Biomimetic 4D printing. Nat. Mater. **15**, 413–418 (2016). https://doi.org/10.1038/nmat4544
141. Taghavi, M., Helps, T., Rossiter, J.: Electro-ribbon actuators and electro-origami robots **9795** (2018)
142. Tang, J., Zhou, Y., Wan, L., Huang, F.: Automatically programmable shape-memory polymers based on asymmetric swelling of bilayer structures. Macromol. Rapid Commun. **39**, 1–7 (2018). https://doi.org/10.1002/marc.201800039
143. Tang, R., Huang, H., Tu, H., et al.: Origami-enabled deformable silicon solar cells. Appl. Phys. Lett. **104** (2014). https://doi.org/10.1063/1.4866145
144. Tao, Y., Gu, J., An, B., et al.: Demonstrating thermorph: democratizing 4D printing of self-folding materials and interfaces. In: Conference on Human Factors in Computing Systems—Proceedings 2018, pp. 1–12 (2018). https://doi.org/10.1145/3170427.3186478
145. Teunis, J.S., Zadpoor, A.A.: Programming 2D/3D shape-shifting with hobbyist 3D printers. Mater. Horiz. **4**, 1064–1069 (2017). https://doi.org/10.1039/c7mh00269f
146. Timoshenko, S.: Analysis of bi-metal thermostats. JOSA **11**, 233–255 (1925)
147. Tolley, M.T., Felton, S.M., Miyashita, S., et al.: Self-folding origami: Shape memory composites activated by uniform heating. Smart Mater. Struct. **23** (2014). https://doi.org/10.1088/0964-1726/23/9/094006
148. Tomatsu, I., Peng, K., Kros, A.: Photoresponsive hydrogels for biomedical applications. Adv. Drug Deliv. Rev. **63**, 1257–1266 (2011). https://doi.org/10.1016/j.addr.2011.06.009
149. Truby, R.L., Lewis, J.A.: Printing soft matter in three dimensions. Nature **540**, 371–378 (2016). https://doi.org/10.1038/nature21003
150. Tu, H., Jiang, H., Yu, H., Xu, Y.: Hybrid silicon-polymer platform for self-locking and self-deploying origami. Appl. Phys. Lett. **103** (2013). https://doi.org/10.1063/1.4842235
151. Tyagi, P., Bassik, N., Leong, T.G., et al.: Self-assembly based on chromium/copper bilayers. J. Microelectromech. Syst. **18**, 784–791 (2009). https://doi.org/10.1109/JMEMS.2009.2023841
152. Vaccaro, P.O., Kubota, K., Aida, T.: Strain-driven self-positioning of micromachined structures. Appl. Phys. Lett. **78**, 2852–2854 (2001). https://doi.org/10.1063/1.1371525
153. Van Honschoten, J.W., Berenschot, J.W., Ondaṛuhu, T., et al.: Elastocapillary fabrication of three-dimensional microstructures. Appl. Phys. Lett. **97** (2010). https://doi.org/10.1063/1.3462302
154. Van Manen, T., Janbaz, S., Zadpoor, A.A.: Programming 2D/3D shape-shifting with hobbyist 3D printers. Mater. Horiz. **4**, 1064–1069 (2017). https://doi.org/10.1039/c7mh00269f
155. Volkov, A.G., Foster, J.C., Ashby, T.A., et al.: Mimosa pudica: electrical and mechanical stimulation of plant movements. Plant Cell Environ. **33**, 163–173 (2010). https://doi.org/10.1111/j.1365-3040.2009.02066.x
156. Wang, E., Desai, M.S., Lee, S.W.: Light-controlled graphene-elastin composite hydrogel actuators. Nano Lett. **13**, 2826–2830 (2013). https://doi.org/10.1021/nl401088b
157. Wang, H., Wang, Y., Tee, B.C.K., et al.: Shape-controlled, self-wrapped carbon nanotube 3D electronics. Adv. Sci. **2** (2015). https://doi.org/10.1002/advs.201500103
158. Wang, M., Lin, B.P., Yang, H.: A plant tendril mimic soft actuator with phototunable bending and chiral twisting motion modes. Nat. Commun. **7**, 1–8 (2016). https://doi.org/10.1038/ncomms13981
159. Whitney, J.P., Sreetharan, P.S., Ma, K.Y., Wood, R.J.: Pop-up book MEMS. J. Micromech. Microeng. **21** (2011). https://doi.org/10.1088/0960-1317/21/11/115021
160. Xu, S., Yan, Z., Jang, K.I., et al.: Assembly of micro/nanomaterials into complex, three-dimensional architectures by compressive buckling. Science (80-) **347**, 154–159 (2015). https://doi.org/10.1126/science.1260960
161. Xu, T., Zhang, J., Salehizadeh, M., et al.: Millimeter-scale flexible robots with programmable three-dimensional magnetization and motions. Sci. Robot. **4** (2019). https://doi.org/10.1126/scirobotics.aav4494
162. Yan, Z., Zhang, F., Liu, F., et al.: Mechanical assembly of complex, 3D mesostructures from releasable multilayers of advanced materials. Sci. Adv. **2** (2016a). https://doi.org/10.1126/sciadv.1601014

163. Yan, Z., Zhang, F., Wang, J., et al.: Controlled mechanical buckling for origami-inspired construction of 3D microstructures in advanced materials. Adv. Funct. Mater. **26**, 2629–2639 (2016). https://doi.org/10.1002/adfm.201504901
164. Yang, Y., Song, X., Li, X., et al.: Recent progress in biomimetic additive manufacturing technology: from materials to functional structures. Adv. Mater. **30**, 1–34 (2018). https://doi.org/10.1002/adma.201706539
165. Yang, Y., You, Z.: Geometry of transformable metamaterials inspired by modular origami. J. Mech. Robot. **10**, 1–10 (2018). https://doi.org/10.1115/1.4038969
166. Yoon, C, Xiao, R., Park, J., et al.: Functional stimuli responsive hydrogel devices by self-folding. Smart Mater. Struct. **23** (2014). https://doi.org/10.1088/0964-1726/23/9/094008
167. Yu, K., Ritchie, A., Mao, Y., et al.: Controlled sequential shape changing components by 3D printing of shape memory polymer multimaterials. Procedia IUTAM **12**, 193–203 (2015). https://doi.org/10.1016/j.piutam.2014.12.021
168. Yuan, C., Roach, D.J., Dunn, C.K., et al.: 3D printed reversible shape changing soft actuators assisted by liquid crystal elastomers. Soft Matter **13**, 5558–5568 (2017). https://doi.org/10.1039/c7sm00759k
169. Zanardi, J.M., Vaccaro, P.O., Fleischmann, T., et al.: Optical actuation of micromirrors fabricated by the micro-origami technique. Appl. Phys. Lett. **83**, 3647–3649 (2003). https://doi.org/10.1063/1.1622800
170. Ze, Q., Kuang, X., Wu, S., et al.: Magnetic shape memory polymers with integrated multifunctional shape manipulations. Adv. Mater. **1906657**, 1–8 (2019). https://doi.org/10.1002/adma.201906657
171. Zhang, X., Li, J., Chen, C., et al.: A self-powered microfluidic origami electrochemiluminescence biosensing platform. Chem. Commun. **49**, 3866–3868 (2013). https://doi.org/10.1039/c3cc40905h
172. Zhao, Y., Nandra, M.S., Tai. Y.C.: A MEMS intraocular origami coil. In: 2011 16th International Solid-State Sensors, Actuators and Microsystems Conference, TRANSDUCERS'11, pp. 2172–2175 (2011). https://doi.org/10.1109/TRANSDUCERS.2011.5969378
173. Zhao, Z., Fang, D., et al.: Origami by frontal photopolymerization. Sci. Adv. **3**, e1602326 (2017a)
174. Zhao, Z., Wu, J., Mu, X., et al.: Desolvation induced origami of photocurable polymers by digit light processing. Macromol. Rapid Commun. **38**, 1–6 (2017). https://doi.org/10.1002/marc.201600625
175. Zhou, X., Li, T., Wang, J., et al.: Mechanochemical regulated origami with tough hydrogels by ion transfer printing. ACS Appl. Mater. Interfaces **10**, 9077–9084 (2018). https://doi.org/10.1021/acsami.8b01610
176. Zhu, Y., Yao, S., Huang, Q., et al.: Controlling the self-folding of a polymer sheet using a local heater: the effect of the polymer–heater interface. Soft Matter **13**, 3863–3870 (2017). https://doi.org/10.1039/c7sm00568g